

# ENERGY | Review of Low-Energy Nuclear Reactions<sup>☆</sup>

SB Krivit, San Rafael, CA, USA

© 2013 Elsevier Inc. All rights reserved.

<b>Introduction</b>	2
<b>History</b>	3
<b>Mechanism</b>	3
Lack of Prompt Radiation and High Neutron Flux	3
Four-Step Process	3
Key Concepts	5
Nucleosynthetic Reaction Chains	6
Gamma Suppression	6
Reaction Rates, Power Density and Energy Density	8
<b>Review of Experimental Methods</b>	9
Basic Steps in LENR Experiments	9
Index of LENR Experimental Methodologies	10
Category: Electrolytic methods	10
Category: Gas methods	13
Category: Unique methods	15
<b>Products and Effects</b>	18
Isotopic Anomalies	18
Energetic Charged Particles	21
Low-Flux Neutron Emissions	21
Neutrons - India	21
Neutrons - USA (SPAWAR)	23
Neutrons - USA (SRI International)	23
Neutrons - Italy	23
Light-Element Transmutations	26
Tritium and helium-3	26
Helium-4	27
Heavy-Element Transmutations	28
Miley's Nickel-hydrogen electrolysis experiments	28
Mizuno's Palladium-deuterium electrolysis experiments	28
Miley-Mizuno-Widom/Larsen's correspondence	29
Iwamura's Gas-permeation experiments	30
Surface Anomalies and Morphological Changes	32
Vaporized metal	32
Hot spots	33
Morphological changes	36
<b>Excess Heat and Calorimetry</b>	44
Excess Heat	44
Palladium-deuterium electrolytic system - IMRA	44
Palladium-deuterium electrolytic system - SRI International	44
Nickel-hydrogen gas-loading and electrolytic systems	44
<b>Calorimetry</b>	46
Isoperibolic calorimetry	46
Mass-flow calorimetry	49
Enclosure calorimetry (Seebeck-type)	50
Isoperibolic-enclosure hybrid calorimetry	50
<b>Calorimetry Critique</b>	50
Improper stirring critique	50
Recombination error critique	51
Low magnitude of heat effect critique	51

<sup>☆</sup>Change History: June 2013. SB Krivit added abstract and has rewritten text.

<b>General Characteristics of Low-Energy Nuclear Reactions</b>	51
Runaway Experiments and Self-Heating	51
Positive Feedback	52
Materials Science Challenges	53
Technology Readiness of LENR	54
<b>Conclusion</b>	54
<b>References</b>	54

### Glossary

**CMNS** (Condensed matter nuclear science), field of study that investigates low-energy nuclear reactions, nuclear effects in or on condensed matter.

**Deuterium** One of three possible isotopes of hydrogen.

**Deuteron** The nucleus of a deuterium atom, comprising one proton and one neutron.

**Heavy water** (D<sub>2</sub>O), water molecules made from deuterium instead of hydrogen.

**Loading ratio** The ratio between deuterium and palladium atoms within a palladium cathode.

**LENRs** Research and experiments that take place at or close to room temperature and pressure that produce nuclear-scale energy and nuclear products. The word “low” refers to the input energies to the reactions; the output energies may

be low or high. The distinction between LENRs and nuclear fusion or nuclear fission stems from the fact that they are based primarily on weak interactions rather than the strong force.

**Neutron-catalyzed reaction** A process in which a nucleus absorbs one or more neutrons, which may produce a different stable isotope or an unstable isotope that can undergo different types of decay processes.

**Sonic implantation** A low-energy nuclear reaction method that uses acoustic cavitation to stimulate low-energy nuclear reactions in or on condensed matter.

**Transmutation** The changing of one element to another by the addition or subtraction of one or more protons.

**Weak interaction** A nuclear reaction in which a neutrino is either emitted or absorbed.

## Introduction

Low-energy nuclear reactions (LENRs) are a set of phenomena that take place under specific conditions on the surfaces of metals in the presence of hydrogen or its isotope, deuterium. The experimental research typically takes place at or close to room temperature and standard pressure and produces a variety of nuclear products, effects and nuclear-scale heat. Perhaps the most extraordinary characteristics of these phenomena are that they do not emit strong fluxes of prompt radiation and that the products are generally stable isotopes. For these reasons, LENRs represent a previously unrecognized class of nuclear reactions. The difference between LENRs and nuclear fusion or nuclear fission stems from the fact that they are based primarily on weak interactions rather than the strong force.

The word “low” in “low-energy nuclear reactions” refers to the input energies that go into the reactions; the output energies may be low or high. The term was chosen by its researchers to distinguish it from the field of high-energy physics, which uses very high temperatures or input energies to create nuclear reactions. Researchers also use the term “condensed-matter nuclear science” when they refer to the field of LENR research.

This article provides a broad technical overview of the LENRs in CMNS. It discusses direct evidence of nuclear phenomena, including isotopic shifts, neutrons, tritium and charged particles. These anomalies suggest untold potential for new technologies, including the transmutation of radioactive waste from nuclear fission reactors into stable isotopes, as well as processes that may provide direct heating or heat to generate electricity. The research also suggests the possibility of the production of rare metals, such as platinum, from abundant metals, such as tungsten and nickel.

The observation of excess heat production – at thousands of times greater power and energy densities than any chemical reaction or solar energy – suggests the extraordinary possibility of a new source of clean nuclear energy based on abundant and globally available raw materials.

LENR experiments are undoubtedly complex, and researchers perform them with a variety of configurations. The inputs – that is, potential reactants – may include (but are not limited to) deuterium in heavy water, deuterium gas, hydrogen in normal water, hydrogen gas, lithium, carbon, platinum, palladium, titanium, nickel, aluminum and tungsten. No radioactive reactants are required, and in general, no radioactive products result.

The field is in its third decade. Throughout the history of this field, would-be entrepreneurs have stated that they have or will soon have practical devices based on LENRs. All of those claims have been premature. Although researchers have learned a lot, the field is still primarily a scientific exploration. The research shows a new field of science that bridges the disciplines of chemistry and physics. Ideally, world-changing technologies will eventually evolve from this field. When that will happen is difficult to predict.

## History

On March 23, 1989, electrochemists Martin Fleischmann and B. Stanley Pons claimed in a press conference at the University of Utah that they had achieved nuclear fusion in a tabletop chemistry experiment. A few weeks later, in a preliminary note published in the *Journal of Electroanalytical Chemistry*, they speculated that “the bulk of the energy release is due to an hitherto-unknown nuclear process or processes.”<sup>1</sup>

Details of the historic event, including video of the press conference, a transcript, the University of Utah press release, and the Steven E. Jones conflict (Brigham Young University) that precipitated the press event, is available at the *New Energy Times* Web site.<sup>2</sup>

Fleischmann and Pons were wrong in their speculation about fusion but correct about a hitherto-unknown nuclear process or processes. By the early 1990s, researchers began to realize that the experimental evidence didn’t fit the description of nuclear fusion, and they began to call the research “low-energy nuclear reactions.” The name is a natural alternative to the field of high-energy physics, which requires high initiation energies to produce nuclear effects. LENRs require only low-energy initiation energies – that is, input energies within the chemical realm. The theoretical energetic outputs of LENRs can get very high, in fact, with comparable energy densities of deuterium-tritium thermonuclear fusion.

LENRs, though not called by that name, were studied as early as the 1920s and were part of the inspiration for Fleischmann’s curiosity. Two American chemists, Clarence E. Irion and Gerald L. Wendt, at an American Chemical Society meeting on March 11, 1922, reported a series of exploding-wire experiments. One of these experiments produced a cubic centimeter of helium from half a milligram of tungsten wire as the result of an intense electrical discharge passed through the wire.<sup>3</sup>

In 1929, Alfred Coehn, a German physics professor at the University of Göttingen, also performed experiments and ran currents across palladium wires in the presence of hydrogen gas.<sup>4</sup> Percy Bridgman, a professor of physics at Harvard, Nobel Prize-winner and teacher of Robert Oppenheimer, an American theoretical physicist who played a key role in the Manhattan project, published studies in the 1930s on cold explosions resulting from the compression and shear of metal lattices.<sup>5</sup> The Coehn and Bridgman works were the particular inspirations for the work Fleischmann and his colleague Pons performed, beginning in the mid-1980s.

## Mechanism

### Lack of Prompt Radiation and High Neutron Flux

The lack of dangerous radiation in LENRs immediately distinguishes the underlying mechanism as an unconventional nuclear reaction. Two kinds of radiation are known to science. Prompt radiation is produced and emitted from its source immediately. When the reaction stops, so does the prompt radiation. In contrast, emissions that continue after the reaction stops are called radioactive decay. For example, nuclear power plants produce materials that undergo long-lived radioactive decay.

Quite unexpectedly, LENR experiments do not emit radiation with the energies and intensities of conventional nuclear reactions, such as those occurring in nuclear power plants.

In LENR experiments, radioactive decay has been reported only in rare situations. Of the prompt forms of radiation, the intensity levels, or flux, have been unusually low in proportion to the energy released. This benevolent feature is largely responsible for the initial difficulty that many people, particularly nuclear physicists, had in accepting LENRs, or, as it was called initially, “cold fusion.”

Had the reactions been caused by thermonuclear fusion, Fleischmann and Pons would have been killed by the intense gamma radiation or neutrons emitted from their experiment. Beyond that, the hundreds of researchers who have performed thousands of experiments without shielding over the last two decades are living testament to the benign emissions from LENRs.

Types of prompt radiations detected include X-ray, gamma ray, energetic charged particles and neutrons. All of these radiations are emitted at very low intensities so they are difficult to measure in LENR experiments. Furthermore, most X-rays and energetic charged particles rarely travel outside of LENR experiments. Nevertheless, measurements of such particles have been made at scientifically significant levels.

### Four-Step Process

In 2006, two researchers, Lewis Larsen and Allan Widom, published a theoretical mechanism that tentatively explains the new phenomena of LENRs.<sup>6</sup> The concept, initially conceived by Larsen, is based on neither fusion nor fission, both of which rely on the strong force, but primarily on weak interactions and the creation of neutrons.

The process can be divided into four basic steps, all of which are based on textbook physics. Larsen and Widom examined a broad array of data and methodically analyzed each step to explain what experimentalists had reported ([Figures 1 and 2](#)).

The first step in the Widom-Larsen theory is the creation of heavy surface plasmon electrons. Groups, or patches, of collectively oscillating protons or deuterons form on metallic hydride surfaces loaded with hydrogen or deuterium. Required conditions include high electromagnetic fields on the surfaces of metal hydrides. The oscillating patches of protons or deuterons begin to couple loosely to nearby surface plasmon electrons. The coupling increases the local electric field to values greater than  $10^{11}$  V m<sup>-1</sup>. As a result of these collective effects, a large number of protons and electrons each contribute a small amount of their energy to a fewer number of electrons, thus adding at least 0.78 MeV to them, and they become heavy surface plasmon electrons.

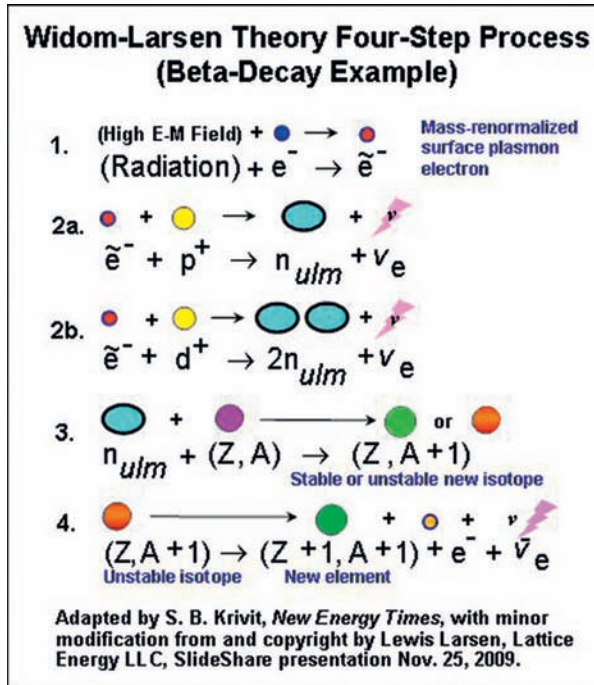


**Figure 1** Four steps of Widom-Larsen theory. Step 2 is listed twice: 2a depicts a normal hydrogen reaction; 2b depicts the same reaction with heavy hydrogen. All steps except the third are weak-interaction processes. Step 3 is a neutron-capture process, a strong interaction.



**Figure 2** Legend to four steps of Widom-Larsen theory.



The second step is the creation of ultra-low-momentum neutrons (ULMN). Once the heavy surface plasmon electrons have the additional 0.78 MeV, they can react spontaneously with nearby protons or deuterons. The heavy surface plasmon electrons and protons undergo inverse beta decay, which is a weak interaction, and create ultra-low-momentum (ULM) neutrons and neutrinos.

In the third step, the ULMN is captured by a nearby nucleus and, through a chain of nuclear reactions, produces a new stable isotope or a new isotope unstable to beta decay. A free neutron outside of an atomic nucleus is unstable to beta decay; it has a half-life of approximately 13 min and decays into a proton, an electron and a neutrino. ULM neutrons have huge quantum mechanical wavelengths (micron-scale), and for this reason, they are almost always absorbed locally by nearby nuclei and are not detected.

In the fourth step, an unstable nucleus beta-decays, and a neutron inside the nucleus decays into a proton, an energetic electron and a neutrino. The energetic electron released in a beta decay exits the nucleus as a beta particle. Because the number of protons in that nucleus has increased by one, the atomic number has increased, creating a different element and transmutation product.

Although the mechanism is often described as the interaction of two particles (a proton and an electron), it is by no means a two-particle reaction. The Widom-Larsen idea that a sea of surface plasmon electrons works collectively on the surface of metallic hydrides in LENRs to create a few heavy surface plasmon electrons is intrinsic to the concept.

The heavy surface plasmon electrons in LENR systems have the unusual ability to absorb gamma photons directly and reradiate them as infrared and soft X-ray photons. As a result, when prompt hard gamma photons are emitted in the reactions from neutron absorption by local nuclei or beta decays, they are intercepted by the heavy surface plasmon electrons and reradiated as much softer electromagnetic energy. This, in effect, is the built-in gamma shield for LENRs and explains why heavy shielding is not required for conducting safe LENR experiments and why no LENR researchers have died from radiation.

### Key Concepts

The idea of using weak interactions to explain the phenomena wasn't a complete surprise to researchers in the field, but most of them, including Fleischmann and Pons, lacked specific expertise in weak interactions. Just three weeks after the Fleischmann-Pons announcement in 1989, Larry A. Hull, in a letter published by *Chemical & Engineering News*, proposed weak interactions and the creation of neutrons to explain the phenomena.<sup>7</sup> Within the next decade, many other researchers also suggested the idea of weak interactions and the creation of neutrons. But not until Larsen figured out precisely how the neutrons are created were he, and later he and Widom, able to figure out a viable LENR mechanism.

Of hundreds of professional and amateur scientists, Widom and Larsen are the only theorists who offer a mechanism that can explain LENRs from start to finish, with complete and correct mathematics. They can also explain their concept in plain English without the use of mathematics. Their theory, unlike nearly every other theory that attempts to explain LENR, does so without relying on imaginary physics. For these reasons, members of the scientific community who had not paid attention to the field in more than a decade began to look at the field with fresh eyes and take it seriously after the Widom-Larsen paper published in 2006.

The initial idea proposed by Fleischmann and Pons that deuterons were overcoming the Coulomb barrier at appreciable rates at room temperature – the hypothetical idea of cold fusion – required too many miracles to be believed. Neutrons, on the other hand, are immune to the Coulomb barrier and require no miracles. However, researchers never saw high rates of neutrons emitted from their experiments. As a result, Larsen realized the neutrons had to have ultra-low momentum, even colder than ultracold neutrons.

Researchers also never saw appreciable gamma emissions from the experiments. The Widom-Larsen theory and a U.S. patent issued to Larsen explain how gamma radiation is suppressed locally, in the micron-scale and smaller regions on the surfaces of the metal hydrides.<sup>8</sup> The suppression mechanism inhibits MeV-range gamma rays from escaping from the immediate vicinity of the reaction sites. The heavy electrons shield the gammas and convert them into infrared radiation, which then becomes a benign source of heat and, therefore, a potential source of clean energy. In addition to heat, the products that are observed and measured include a variety of nuclear transmutations. In general, according to both experimental observations and the Widom-Larsen theory, the nucleosynthetic reaction chains terminate in stable isotopes.

Energy may be released through neutron-capture processes (creating gamma rays that are converted into infra-red heat by nearby heavy electrons), alpha decays, beta decays, beta-delayed neutron emissions and beta-delayed alpha decays, among others. Different values of energy release are associated with each process and each set of particles involved in the reaction network.

The Widom-Larsen theory relies heavily on modern electroweak theory, also known as quantum electrodynamics, which addresses the behavior of particles in fields. A key piece of the puzzle is that the normal assumption that the Born-Oppenheimer approximation, normally used as a mathematical shortcut to perform basic quantum mechanics calculations, does not apply in this case.

There are six key concepts of the Widom-Larsen explanation of the LENR mechanism:

- Quantum electrodynamics is intrinsic to the mechanism.
- LENRs are primarily a surface rather than bulk effect.
- Collective, many-body effects are essential in making the heavy electrons.
- Ultra-low-momentum neutrons are created.
- Subsequent neutron-capture processes create the isotopic and elemental changes.
- Gamma radiation is converted to infrared radiation locally, at the surface.
- The Born-Oppenheimer approximation breaks down.

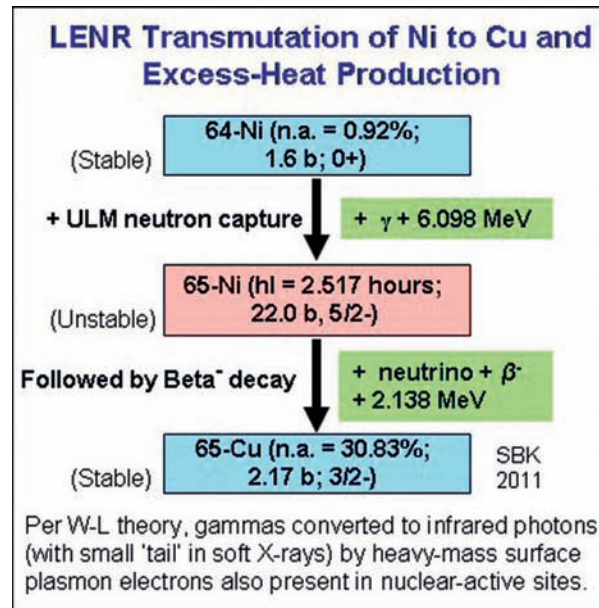


**Figure 3** Nucleosynthetic reaction chain example of Ni-64 transmutation to Cu-65.<sup>6,9,10</sup>

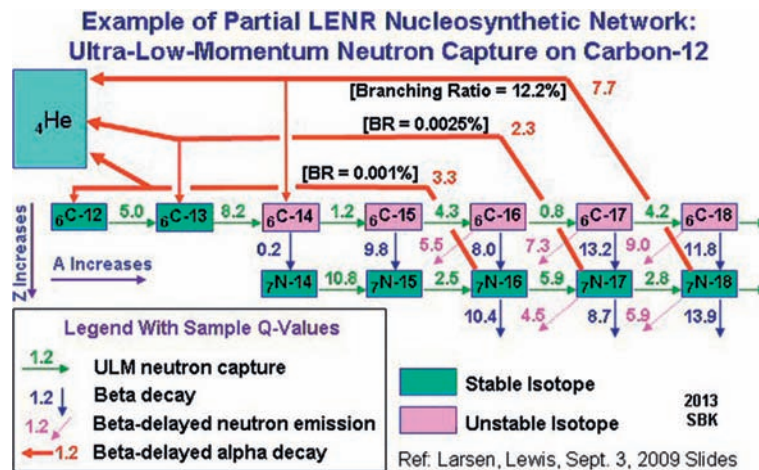


**Figure 4** Nucleosynthetic reaction chain example of C-12 transmutation to He-4.

### Nucleosynthetic Reaction Chains

Once neutrons are created in the system, a variety of nucleosynthetic reaction chains may occur. [Figures 3 and 4](#) show two examples of possible reaction chains.

### Gamma Suppression

Any kind of fusion or neutron-capture reaction that produces significant heat should emit enough gamma radiation to kill anyone in its vicinity. Throughout the history of this field, critics have wondered, If it's really nuclear, then where are the gammas? On March 22, 2013, Larsen published a slide presentation that explains why deadly gamma radiation is not emitted in LENRs.<sup>11</sup>

Two paragraphs in his slides contain the key text that explains the gamma suppression for prompt gammas. It is excerpted below and edited slightly for clarity.

"When an ultra-low-momentum neutron captures onto an atom located inside the entangled three-dimensional quantum-mechanical structure of a LENR-active patch, there is normally a prompt gamma photon emission by that atom," Larsen wrote. "The key point to remember is that the DeBroglie wave functions of the entangled, mass-renormalized heavy electrons are also three-dimensional, not two-dimensional. [The surface of a metal hydride is not two-dimensional; it has some depth.]" Larsen said:

Because the neutron-capture gamma photon emission occurs within the structure of a LENR-active patch, there are always heavy electrons available nearby to absorb such gamma emissions and convert them directly into infrared photons. Therefore, it doesn't matter where a gamma emission occurs inside a given patch; it will always get converted to infrared, which is exactly what has been observed experimentally. Large fluxes of hard gammas will not be emitted from such a patch, no matter which direction, on any axis, they are measured from.

In his slides, Larsen also explains the gamma suppression that occurs with beta-delayed gammas that can occur in the reactions.

Larsen also discusses an experiment performed by the Francesco Piantelli group in the 1990s.<sup>12,13</sup> One of the group's key experiments ran for many weeks and produced significant excess heat. According to the Widom-Larsen theory, gamma emissions above 0.5 to 1.0 MeV are suppressed.

In the larger graph below (Figure 5), the black line shows the background gamma counts, and the red line shows the measured gamma counts from the experiment. Background gamma counts go out to 2500 in a slowly decreasing curve. The net measured photon radiation, shown in the inset panel, drop abruptly to background levels at 800 keV.

After the experiment has run for five days (Figure 6), two small gamma peaks are visible, one at about 600 keV and another just below 1500 keV.

After the Piantelli group took the mean of 18 acquisitions during the period from day 6 to day 50 (Figure 7), two remarkable things appear. First, the peak at 600 keV drops from 300 counts to 50. Second, the peak at 1500 keV disappears. No gamma

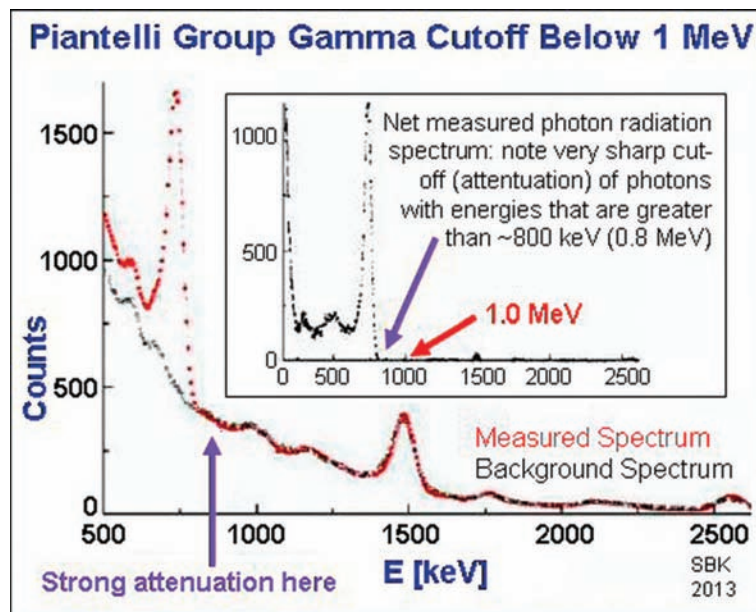


Figure 5 Larsen's annotation of Piantelli's gamma cutoff.<sup>11,14</sup>

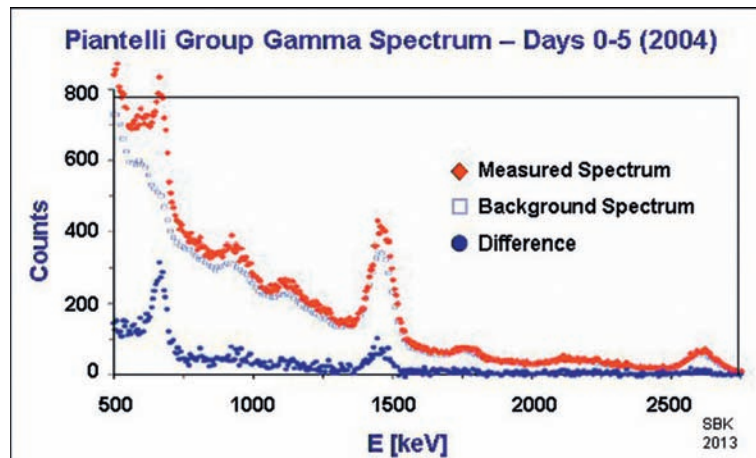
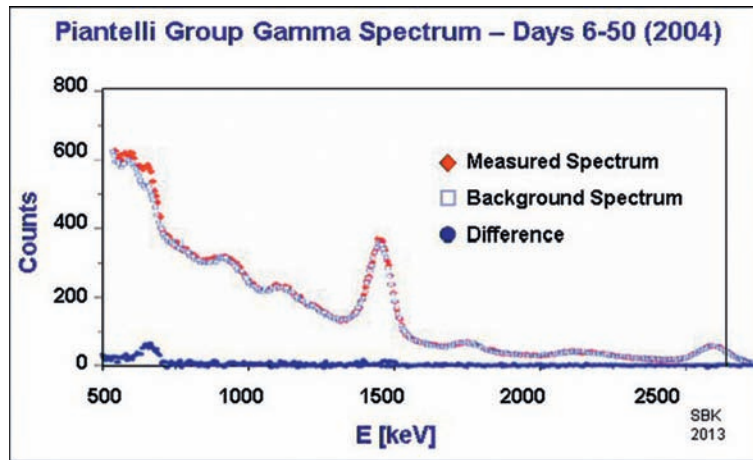


Figure 6 Piantelli group's gamma spectrum, days 0–5.



**Figure 7** Piantelli group's gamma spectrum, days 6–50.

radiation is seen beyond the small peak at 600 keV during this time. This is particularly significant because neutron captures on nickel isotopes normally produce gamma emissions in the MeV range.

"This is a direct experimental observation of the suppression of gammas via conversion to infrared by heavy electrons per our theory," Larsen said. "After 600 keV, the gamma emissions drop off drastically, right on the edge of the cutoff region around 500 to 1000 keV that we predict. All gamma emissions with higher energy than this region drop to background and stay there through the duration of the experiment. Our theory predicts that the suppression also extends up to between 10 and 11 MeV. There are only a handful of other neutron captures, out of thousands, that are more energetic than 11 MeV."

The Piantelli group wrote that, after day 50, the entire gamma spectrum went completely to background and stayed at that level while the experiment continued for another 35 days, during which it produced 25 MJ of heat.<sup>14</sup>

"After this time period," the group wrote, "the spectrum went abruptly to the background one. Later on, the cell produced excess power, maximum 25 W measured with the method reported in Ref. 2, for about 35 days, after which the cell was shut down, in order to repeat the experiment."

In the history of the field, intermittent, low levels of gamma radiation have been reported often. Until now, there was never any logical explanation.

"This is an example of an experiment that produced a huge amount of heat," Larsen said. "Initially, you don't have a large population of heavy electrons. But once you start making them, which are required to start making the heat, the gamma is cut off; you get the heat but no gammas." Larsen said:

Some people are thinking the gamma shield is something that is covering the whole surface. This isn't necessary, and this isn't what happens. All you need to do is have the shield at the LENR-active sites. It's intrinsic to the system; the LENR-active sites have their own built-in gamma shield.

### Reaction Rates, Power Density and Energy Density

Widom and Larsen's 2007 paper "Theoretical Standard Model Rates of Proton-to-Neutron Conversions Near Metallic Hydride Surfaces" provides calculations that show LENRs have the potential for practical energy production.<sup>15</sup> In his June 25, 2009, slide presentation, Larsen provides a specific calculation.<sup>16</sup>

Larsen begins with the basic fuel required to produce the neutrons: either hydrogen or deuterium. It costs 0.78 MeV to create the heavy-mass surface plasmon electron. Only one heavy-mass surface plasmon electron is required to produce a neutron for each proton. If the fuel is deuterium or tritium, then the heavy-mass surface plasmon electron reacts with a deuteron or triton and produces either two or three neutrons, respectively.

Therefore, in the case of protium, it costs 0.78 MeV to produce each neutron; for deuterium, 0.39 MeV, and for tritium, 0.26 MeV. In all cases, the neutrons are created by way of a direct electroweak reaction with a heavy-mass surface plasmon electron.

Once a LENR reaction chain begins, a variety of nuclear processes, as mentioned above, release energy. Each beta decay, for example, may release just a few keVs to about 20 MeV of heat. Larsen's review of experimental work also reveals that high implicit neutron production rates are well-correlated with heat generation, as he wrote in an article for the *Institute of Science in Society*.<sup>17</sup>

"In numerous experiments involving well-performing electrolytic LENR cells, with either light or heavy water, LENR production rates on the order of  $1 \times 10^{11}$  to as high as  $1 \times 10^{16}$  per second have been measured with reasonable precision," Larsen wrote. "These values for reaction rates hold true whether the LENR transmutation products are in the form of helium-4 or the complex arrays of different-mass isotopic products such as those found in the experiments of [George] Miley and [Tadahiko] Mizuno."

Larsen's theoretical calculations assume an idealized system of perfect efficiency and establish a theoretical upper bound on a potential energy release from a deuterium-based LENR device with a working surface area of  $1 \text{ cm}^2$ . In the example, Larsen's calculations were based on an assumed rate of approximately  $10^{14}$  reactions  $\text{cm}^2 \text{ s}^{-1}$ , each releasing 26.9 MeV of heat above and



LENRs Versus Chemical Energy Sources: Batteries, Fuel Cells, and Microgenerators	
Source of Energy	Approximate Energy Density (Watt*hours/kg)
Alkaline Battery	164
Lithium Battery	329
Zinc-Air Battery	460
Direct Methanol Fuel Cell (35% efficient)	1,680
Gas Burning Microgenerator (20% efficient)	2,300
100% Efficient Combustion of Pure Methanol	5,930
100% Efficient Combustion of Pure Gasoline	11,500
LENRs (based on an assumption of an average of 0.5 MeV per nuclear reaction in an LENR system)	57,500,000 (maximum theoretical energy density – only a fraction would be achievable in practice)

**Figure 8** Slide from Larsen's September 27, 2011, slide presentation showing approximate comparative energy densities. Image courtesy Lewis Larsen and Lattice Energy LLC.

beyond the energy to create the neutrons. The theoretical upper bound on total heat production amounts to 34 times the input power; Larsen calculated the surface area power density of this hypothetical LENR-based device to be  $428 \text{ W cm}^{-2}$ .

Scaling up total surface area of a LENR-based thermal source from a square centimeter to a square meter – a 10,000-fold increase – would provide a 4.28 MW power source. This area density of thermal power output can be compared to the maximum amount of solar power reaching the Earth's surface, which is about  $0.001 \text{ MW m}^{-2}$ , a difference of 4000 times. The area thermal power densities potentially achievable with LENR technology are thus vastly larger than any competing power generation technology based on capture and conversion of energy from incident solar photons of various wavelengths.

In his Sept. 27, 2011, slide presentation, Larsen made an estimate of potential LENR energy density, as well. He took a conservative value of an average of 0.5 MeV per nuclear reaction and compared that to the approximate energy density of gasoline (Figure 8).<sup>18</sup>

For pure gasoline, at 100 percent combustion efficiency, he calculates an approximate energy density of  $11,500 \text{ Wh kg}^{-1}$ . For the 0.5 MeV LENR reaction, he calculates an approximate energy density of  $57,500,000 \text{ Wh kg}^{-1}$ . That's 5000 the energy density of gasoline. Larsen writes that this is the maximum theoretical energy density and that, in practice, only a fraction of this would be achievable. The question of how long a given LENR fuel will produce power directly factors into its effective energy density and is difficult to determine at this time.

## Review of Experimental Methods

### Basic Steps in LENR Experiments

In 1991, Mahadeva Srinivasan made a list of the basic steps involved in most LENR experiments. Two decades later, the essential steps are the same and apply to most of the methods. Here is his list, slightly edited:

1. Choice of experimental method.
2. Choice of host metal/alloy: Pd, Ni, Ti, Zr, Mg, V, Nb, Ti, any hydrogen-storing alloy; even a high-temperature superconductor.
3. Preparation of samples: degassing, surface cleaning, annealing.
4. Choice of and loading of deuterium/hydrogen: electrolysis, gas, plasma, ion implantation, etc.
5. Measurement of degree of deuterium/hydrogen loading (or D(H)-to-metal atomic ratio): weighing, volume increase, resistivity, X-ray diffraction, etc.
6. Stimulation/triggering of reactions to create non-equilibrium conditions: current pulsing, thermal cycling, electrical discharge, application of electric or magnetic field, pressure changes, ultrasound, low-power laser, shock wave, projectile impact, etc. In many cases, particularly with electrolysis, anomalies do not occur when the system is in equilibrium.
7. On-line diagnostic analyses: heat, neutrons, X-rays, helium-4 (online), gamma rays, thermal imaging, acoustic or pressure waves, radio emissions.
8. Off-line diagnostics or post-experiment analysis: Isotopic anomalies, elemental changes, charged particles, neutrons via CR-39 with or without absorber, helium-4 (offline), helium-3, tritium.
9. Theoretical interpretation, modeling, analysis.

### Index of LENR Experimental Methodologies

Low-energy nuclear reaction researchers have used at least two dozen methods to perform LENR experiments. This index, developed by *New Energy Times*, describes the more common methods (Figures 9–28).

In the 1920s, when researchers searched primarily for transmutations, the typical experimental method they used was a high electric current rapidly introduced to a thin wire, causing it to explode.

When Fleischmann and Pons reinvigorated the field in 1989 and searched primarily for excess heat, they used low-voltage electrolysis. Several months later, Piantelli developed an alternative method of loading hydrogen gas onto the surface of metals. Other researchers, as shown below, developed their own innovative approaches.

Low-voltage electrolysis has been a favorite for its relative simplicity and low cost, but it has been the least successful in producing repeatable results and in proving a nuclear effect. Searches for excess heat are enticing and may get the attention of entrepreneurs because the heat may eventually lead to needed practical applications. However, heat is evanescent and makes a difficult proof for nuclear phenomena; in addition, heat teaches little about the nuclear mechanism.

On the other hand, searches for isotopic or elemental changes provide direct information about the mechanism and produce long-lasting nuclear evidence. Researchers who have conducted experiments in attempts to find isotopic or elemental changes have found that such experiments work more repeatably and more reproducibly.

The comprehensive Widom-Larsen theory of LENRs enables the following varied experimental methods and their results to be understood within a common conceptual framework. Among these methods listed below, an even more diverse collection of protocols and instrumentation choices exist for many of them.

#### Category: Electrolytic methods

See Tables 1–8.

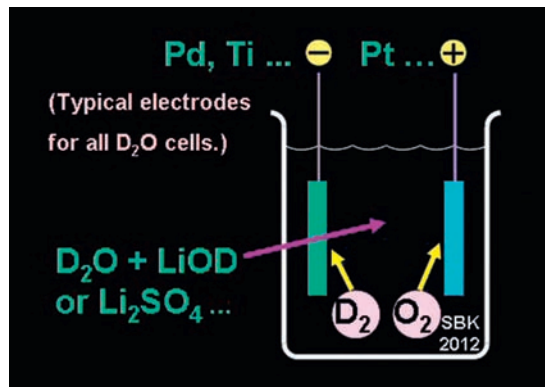


Figure 9 Electrolysis in heavy water.

Table 1 Electrolysis in heavy water

Author Example	Pons and Fleischmann <sup>19</sup>
Typical Configuration	Low-power electrolysis. Pd or Ti cathodes. Pt anodes. D <sub>2</sub> O with LiOD or Li <sub>2</sub> SO <sub>4</sub> .
Typical input power	Less than 5 W
Typical duration	Weeks to months
Typical Search	Excess heat

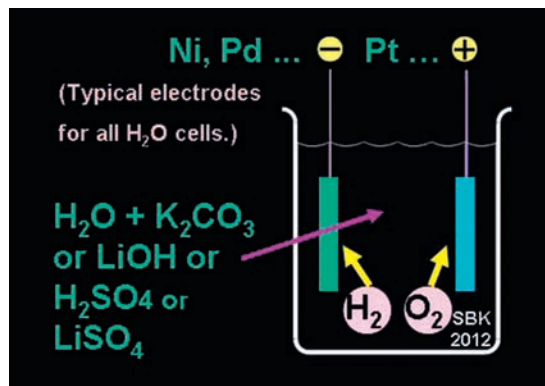
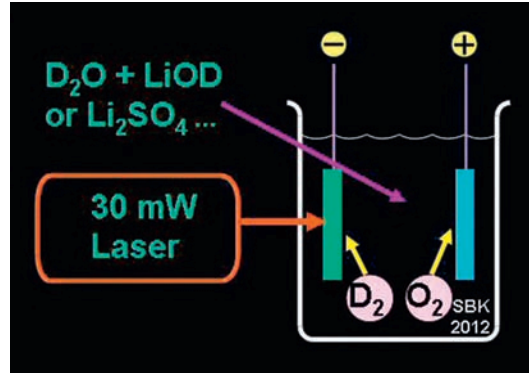


Figure 10 Electrolysis in light water.

**Table 2** Electrolysis in light water

Author Example	Miley, <sup>20</sup> Dash <sup>21</sup>
Typical Configuration	Low-power electrolysis. Ni cathodes. Pt anodes. H <sub>2</sub> O with K <sub>2</sub> CO <sub>3</sub> , LiOH or LiSO <sub>4</sub> or H <sub>2</sub> SO <sub>4</sub> .
Typical input power	Less than 5 W
Typical duration	Days to weeks
Typical Search	Excess heat, nuclear emissions and transmutations



**Figure 11** Electrolysis with low-power laser.

**Table 3** Electrolysis with low-power laser

Author Example	Letts and Cravens, <sup>22</sup> Violante <sup>23</sup>
Typical Configuration	Variation of low-power electrolytic experiment. Addition of ~30 mW laser beam amplifies excess-heat effect.
Typical input power	Less than 5 W
Typical duration	Days to weeks
Typical Search	Excess heat

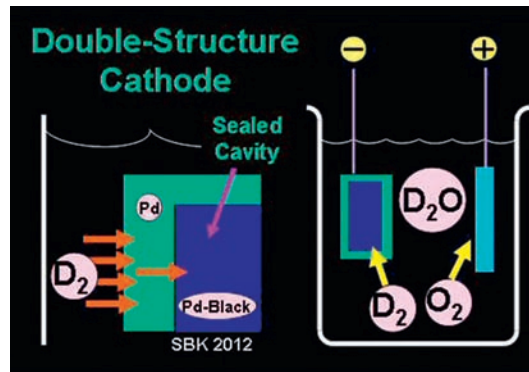


**Figure 12** Electrodiffusion with double-structure cathode.

**Table 4** Electrodiffusion with double-structure cathode

Author Example	Arata and Zhang <sup>24</sup>
Typical Configuration	Low-power electrolysis. Deuterium in D <sub>2</sub> O diffuses through the walls of a hollowed-out (double-structure) cathode filled with Pd-black powder. D <sub>2</sub> gas permeates cathode walls.
Typical input power	100 W
Typical duration	Days to weeks
Typical Search	Excess heat, 4He

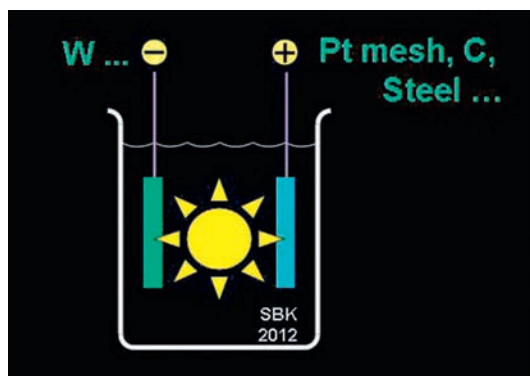


**Figure 13** High-voltage plasma electrolysis in  $D_2O$  or  $H_2O$ .

**Table 5** High-voltage plasma electrolysis in  $D_2O$  or  $H_2O$

Author Example	Mizuno, <sup>25</sup> Cirillo <sup>26</sup>
Typical Configuration	High-power electrolysis causes plasma formation. W cathodes. Anodes can be Pt mesh, carbon, steel. $D_2O$ with LiOD or $H_2O$ with any of LiOH, KOH, NaOH, $K_2CO_3$ , $Na_2SO_4$ , $Na_2CO_3$ , $H_2SO_4$ .
Typical input power	100–800 W
Typical duration	Minutes to hours
Typical Search	Excess heat, nuclear emissions and transmutations

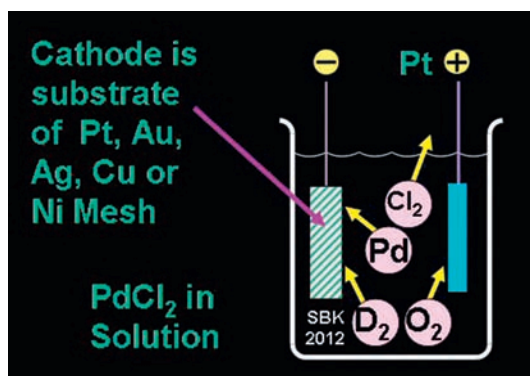


**Figure 14** Electrolytic co-deposition.

**Table 6** Electrolytic co-deposition

Author Example	Mosier-Boss, <sup>27</sup> Miles <sup>28</sup>
Typical Configuration	Cathodes are substrates of Au, Ag or Pt. Anode is Pt. Solutions of $PdCl_2$ and LiCl are added to $D_2O$ . Pd is deposited onto cathode in the presence of evolving $D_2$ .
Typical input power	Less than 5 W
Typical duration	Days
Typical Search	Excess heat, energetic particles, neutrons

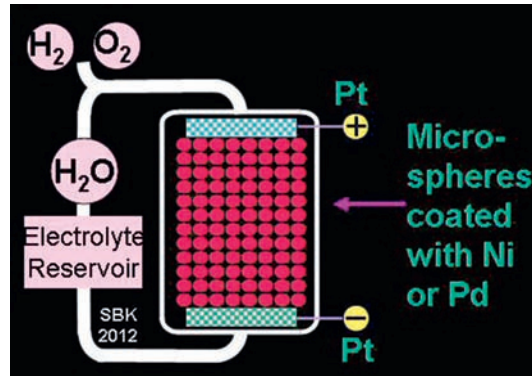


**Figure 15** Thin-film electrolysis in packed bed.

**Table 7** Thin-film electrolysis in packed bed

Author Example	Patterson and Miley <sup>29</sup>
Typical Configuration	Low-power electrolysis. A bed of microspheres coated with Ni or Pd, or both, are immersed in the electrolyte and compose the cathode. Pt cathodes. H <sub>2</sub> O with K <sub>2</sub> CO <sub>3</sub> , LiOH or LiSO <sub>4</sub> .
Typical input power	Less than 5 W
Typical duration	Hours to days
Typical Search	Excess heat, nuclear emissions and transmutations

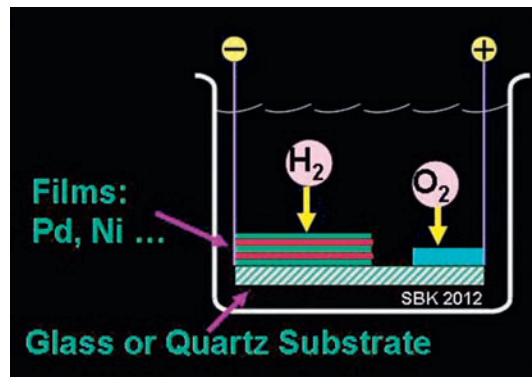


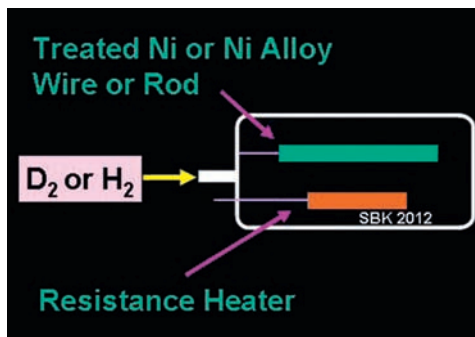
**Figure 16** Thin-film electrolysis on substrate.

**Table 8** Thin-film electrolysis on substrate

Author Example	Miley <sup>30</sup>
Typical Configuration	Glass/Quartz substrate. Cathode consists of multiple layers of Pd, Ni and other materials. Pt anode
Typical input power	Less than 5 W
Typical duration	Hours to days
Typical Search	Excess heat, nuclear emissions and transmutations

**Category: Gas methods**

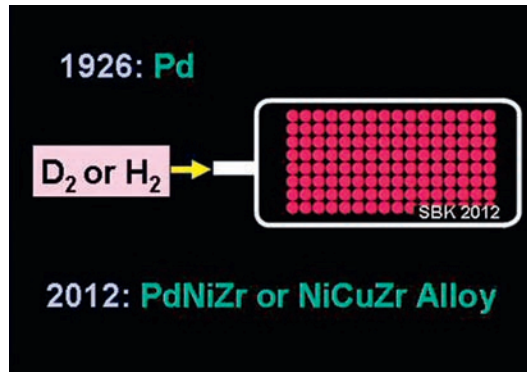
See [Tables 9–13](#).



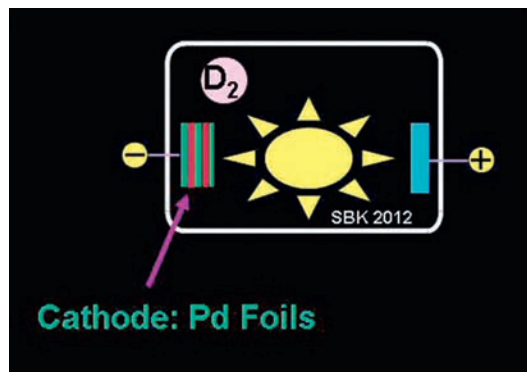
**Figure 17** Gas loading on bulk metal (rod or wire).

**Table 9** Gas loading on bulk metal (rod or wire)

Author Example	Piantelli <sup>14</sup>
Typical Configuration	Pure nickel, nickel alloys or nickel-plated bars are placed in ultra-high-vacuum chamber, which is then filled with hydrogen gas. Initial heating is by resistance and gradually reduced as LENR heating increases.
Typical input power	Tens of Watts
Typical duration	Weeks to months
Typical Search	Excess heat, nuclear emissions and transmutations

**Figure 18** Gas absorption into metal nano-powder.**Table 10** Gas absorption into metal nano-powder

Author Example	Paneth and Peters, <sup>31</sup> Arata <sup>32</sup>
Typical Configuration	Deuterium or hydrogen gas loads into a chamber filled with finely divided palladium or palladium nanopowder.
Typical input power	Only pump power
Typical duration	Days
Typical Search	Search for transmutation, excess heat and helium-4

**Figure 19** Gas plasma - glow discharge.**Table 11** Gas plasma - glow discharge

Author Example	Savvatimova <sup>33,34</sup>
Typical Configuration	Voltage applied to a chamber filled with deuterium or hydrogen gas, or a mixture, plus Ar, Xe, causes a plasma to form
Typical input power	500–1000 volts, 10–100 mA, (5–100 W)
Typical duration	1–40 h
Typical Search	Excess heat, nuclear emissions and transmutations

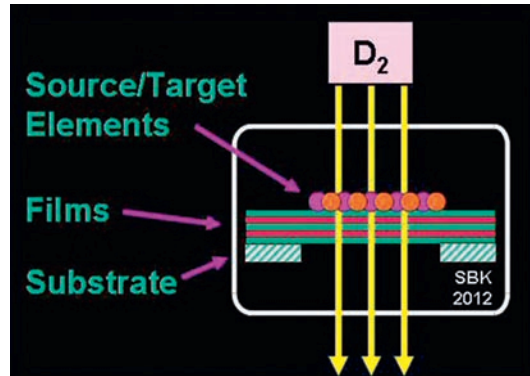


**Figure 20** Gas permeation through thin films.

**Table 12** Gas permeation through thin films

Author Example	Iwamura, <sup>35</sup> Higashiyama <sup>36</sup>
Typical Configuration	Deuterium gas drawn through multi-layer substrates containing palladium and target elements.
Typical input power	Pump power and small electric heater, Pump: 400 W Heater: 10 W
Typical duration	10 days
Typical Search	Search for nuclear emissions and transmutations

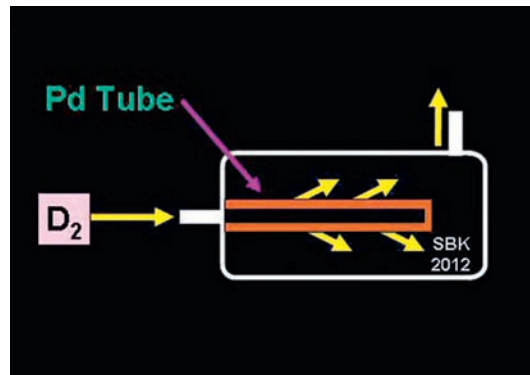


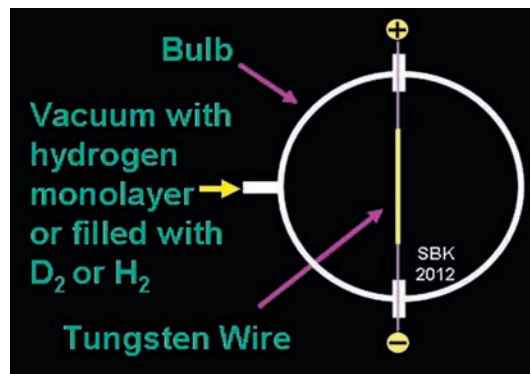
**Figure 21** Gas permeation through thin metals.

**Table 13** Gas permeation through thin metals

Author Example	Biberian, <sup>37</sup> Fralick <sup>38</sup>
Typical Configuration	Deuterium or hydrogen gas is drawn through and loaded into or deloaded from thin sheets or tubes of palladium.
Typical input power	Only pump power
Typical duration	Days
Typical Search	Excess heat, nuclear emissions

**Category: Unique methods**

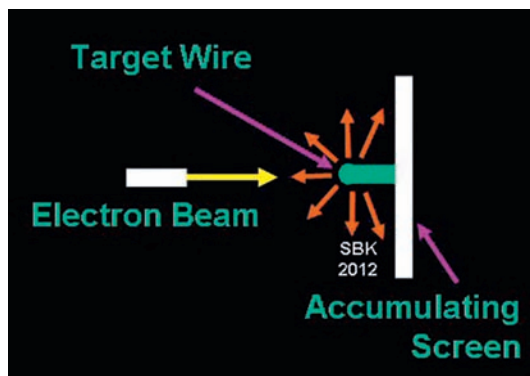
See [Tables 14–20](#).



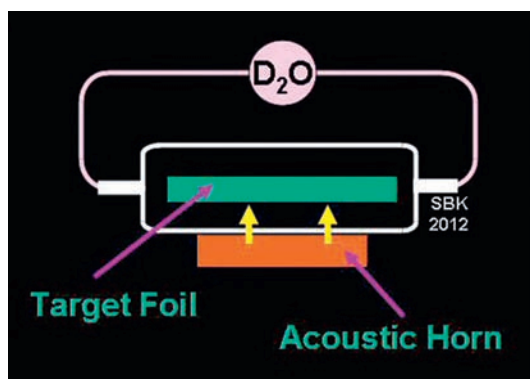
**Figure 22** Exploding wires.

**Table 14** Exploding wires

Author Example	Wendt and Irion, <sup>3</sup> Kortkhonja <sup>39</sup>
Typical Configuration	A high electric current is rapidly introduced to a thin wire. The wire disintegrates in a brilliant flash.
Typical input power	Tens or hundreds of Watts
Typical duration	Seconds to minutes
Typical Search	Nuclear emissions and transmutations

**Figure 23** Electron beam impact.**Table 15** Electron beam impact<sup>40,41</sup>

Author Example	Adamenko, Novikov
Typical Configuration	Bombarding a target metal with high, short-pulse electron current
Typical input power	Power of beam: 200–2000 J; Absorbed by a target: 20–400 J
Typical duration	15–100 ns
Typical Search	Nuclear emissions and transmutations

**Figure 24** Sonic implantation.**Table 16** Sonic implantation

Author Example	Stringham <sup>42</sup>
Typical Configuration	Acoustic waves are directed into an aqueous solution of D <sub>2</sub> O in the presence of a target metal. Bubbles form and collapse at the surface of the metal.
Typical input power	16 W
Typical duration	Hours
Typical Search	Excess heat and helium-4



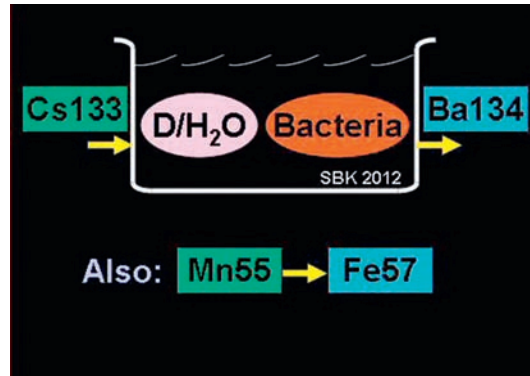


Figure 25 Biological processes.

Table 17 Biological processes

Author Example	Vysotskii and Kornilova <sup>43</sup>
Typical Configuration	Dissolve MnSO <sub>4</sub> in D <sub>2</sub> O or H <sub>2</sub> O containing bacteria. Rare iron isotope Fe57 produced and detected by gamma ray detection, Mossbauer method and TIMS mass-spectroscopy (synchronization of decrease of Mn55 concentration and increase of Fe57 concentration).
Typical input power	None
Typical duration	24–72 h for the case of “online” (“clean”) microbiological cultures like Escherichia coli (low efficiency of transmutation) and 50–100 days for microbe syntrophin association of thousands kinds of microbiological cultures (high efficiency of transmutation)
Typical Search	Nuclear transmutations of stable (e.g. Mn55 to Fe57) and radioactive (e.g. Cs137 to Ba138) isotopes.

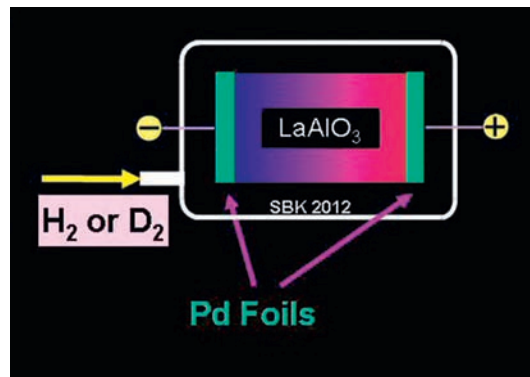
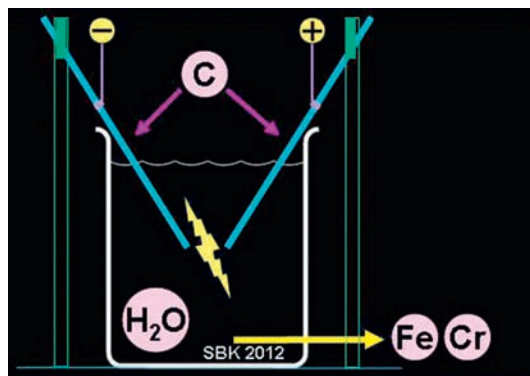


Figure 26 Electromigration through solid-state proton conductors.

Table 18 Electromigration through solid-state proton conductors

Author Example	Mizuno, <sup>44</sup> Biberian <sup>45</sup>
Typical Configuration	Hydrogen or deuterium atoms caused to move across solid material when voltage is applied.
Typical input power	100 mW–10 W
Typical duration	Minutes to hours
Typical Search	Excess heat



**Figure 27** Carbon arc experiments.

**Table 19** Carbon arc experiments

Author Example	Sundaresan and Bockris <sup>46</sup>
Typical Configuration	Carbon rods suspended in H <sub>2</sub> O. Transmutations found in detritus.
Typical input power	10–30 A
Typical duration	Hours
Typical Search	Excess heat, nuclear emissions and transmutations

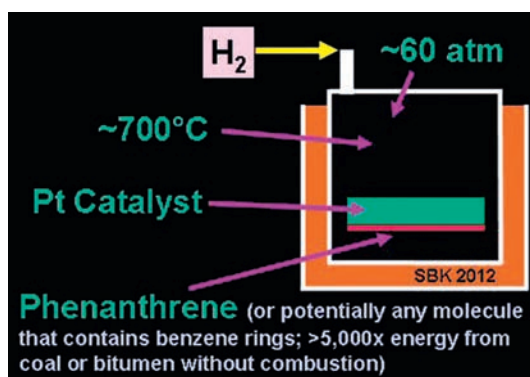


**Figure 28** Hydrogen loading of phenanthrene.

**Table 20** Hydrogen loading of phenanthrene

Author Example	Mizuno <sup>47</sup>
Typical Configuration	Heavy oil is heated in high-pressure hydrogen gas with a metal catalyzer.
Typical input power	500–1000 W
Typical duration	Hours
Typical Search	Excess heat, nuclear emissions and transmutations

## Products and Effects

### Isotopic Anomalies

Reports of anomalous isotopic abundances in LENR experiments have been reported in the field for two decades. [Figure 29](#) represents the changes to the palladium isotopic ratios that took place as the result of a heavy-water LENR electrolysis experiment performed by researcher Tadahiko Mizuno in 1991. A variety of significant changes is evident. [Figure 30](#), from the same experiment, also shows a significant anomalous shift in the isotopes of chromium.<sup>48</sup>

Yasuhiro Iwamura and co-workers at Mitsubishi Heavy Industries in Japan have also reported many anomalous isotopic shifts as well as heavy-element transmutations in their palladium-deuterium gas permeation method.<sup>35</sup>

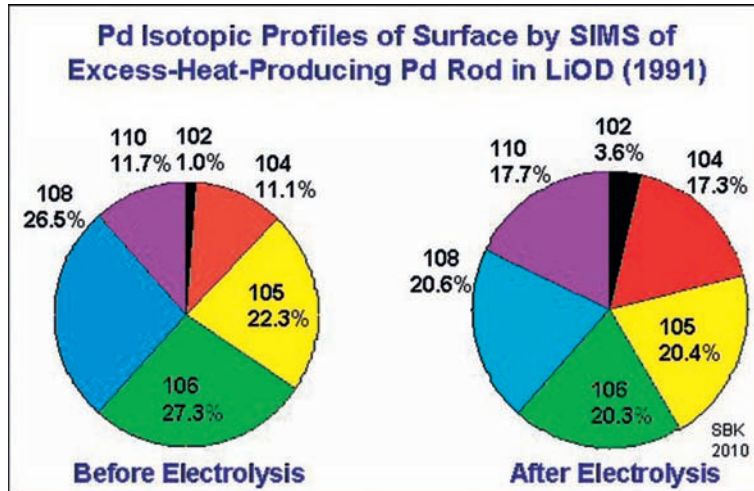


Figure 29 Changes to palladium isotopic ratios.

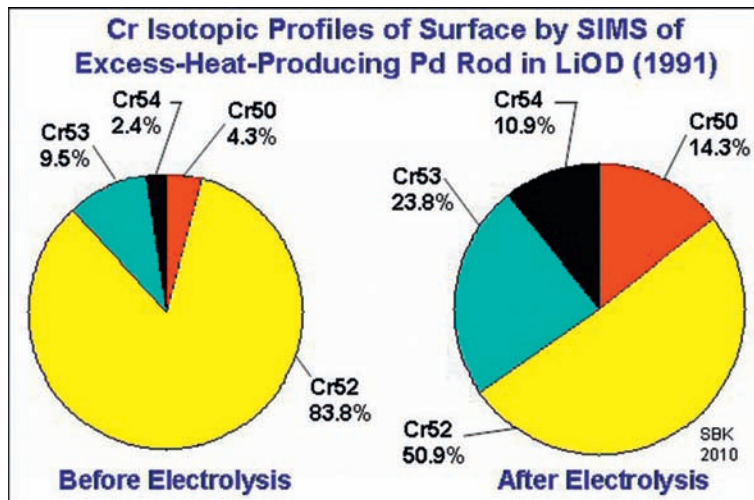


Figure 30 Changes to chromium isotopic ratios.

Images below (Figures 31 and 32) show a significant change after the experiment in isotopic abundances of Mo from the natural abundance. Iwamura confirmed the detected Pr by a variety of methods, including TOF-SIMS, XANES, X-ray Fluorescence Spectrometry and ICP-MS.

In November 1999, Thomas Passell, a former program manager at the Electric Power Research Institute, reported isotopic shifts from a cathode (palladium rod) that had been used by Pons in a set of heavy-water electrolysis experiments that generated lots of excess heat.<sup>49</sup> The authors of the report wrote, based on their understanding of nuclear chemistry, that “the excess power episodes observed with the cathode integrated over the time of the episodes must have totaled 160 kJ.” This was their most conservative estimate.

“Pons of IMRA volunteered a cathode that had experienced such episodes of excess heat well above the required levels of several hundred kilojoules,” the researchers wrote. “It was this cathode and its virgin counterpart that were analyzed in this study.”

The researchers showed that, by the most conservative estimate of nuclear binding energy released by the isotopic shift, Pons’ experiment produced an amount of heat in good agreement with the excess heat Pons measured.

Pons had not provided the precise amounts of excess heat produced by this cathode, but in a similar experiment from 1996, he reported that the palladium-deuterium experiment produced 101 W of excess heat for 30 days, giving 294 MJ of excess energy.<sup>19</sup>

Passell and his colleagues at the University of Texas back-calculated the minimum amount of energy release, based on the facts they obtained from the NAA along with their knowledge of nuclear binding energy. They based their interpolation on the most conservative estimate of depleted Pd-110 atoms (7%), and from this, they extrapolated an amount of energy in approximate agreement with that which Pons had reported by his calorimetry.

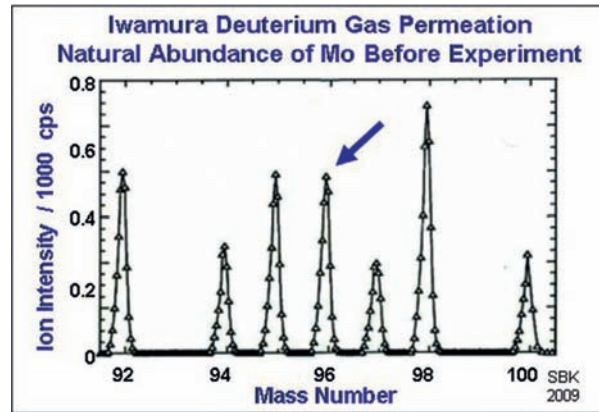


**Figure 31** Iwamura and Itoh's Mitsubishi Heavy Industries experiment. SIMS measurement of natural Mo before performing D<sub>2</sub> gas-diffusion experiment. Several Mo isotopes are abundant.

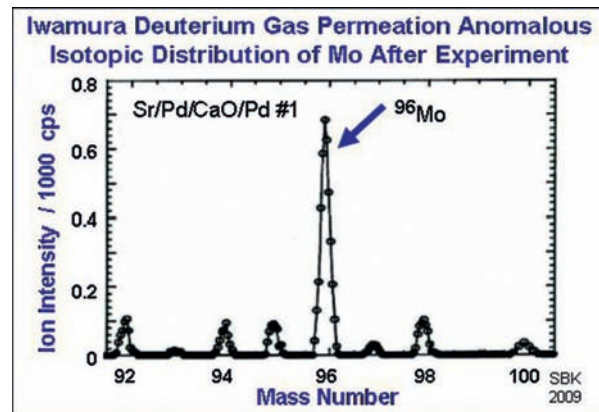


**Figure 32** Iwamura and Itoh's Mitsubishi Heavy Industries gas-permeation experiment. SIMS measurement of anomalous isotopic abundances of Mo after performing D<sub>2</sub> gas-diffusion experiment.

Passell and another EPRI program manager, Albert Machiels, explained their calculations.

"If we take the 7% number as the value, this implies a loss of  $2.3 \times 10^{18}$  atoms of Pd-108," Passell and Machiels wrote. "At 10 MeV per atom lost, this amounts to 3.6 MJ for the sample, and extrapolating to the total cathode, assuming homogeneity, gives 163 MJ of excess heat. Of course, total homogeneity is not likely in the electrochemical cell. The total excess heat generated by this cathode has not been made available to us as yet." Passell wrote:

To get 163 MJ of excess heat would require an episode with an excess power of 10 W for 4527 h, or about 0.5 years. The conclusion we must draw is that homogeneity is unlikely for excess-heat episodes or that our measurement of Pd-108 depletion is in error. However, it should be noted that Roulette, Roulette, and Pons report one cell giving a total net excess heat of 294 MJ and another yielding 102 MJ.

The University of Texas analysis (Table 21) shows a variety of transmutations in the cathode. The researchers reported 4 times the amount of cobalt (Co), 5.4 times the amount of chromium (Cr), 2 times the amount of cesium (Cs), 1.3 times the amount of europium (Eu), 56 times the amount of iron (Fe) and 11 times the amount of zinc (Zn) that is found in the virgin material.

Passell performed a similar analysis on a sample from a palladium-deuterium experiment by Yoshiaki Arata and Yue-Chang Zhang. The analysis showed an increase of 6.6 to 14.4 times the Zn-64 isotope over the virgin palladium.<sup>50</sup>

Passell estimated that the nuclear binding energy released by the production of the excess Zn-64 would be 20 MJ, which is in approximate agreement with the 30–40 MJ of excess heat Arata and Zhang measured in similar experiments. Arata analyzed for helium-4 but not for isotopic shifts.

Passell worked with the University of Missouri to perform prompt gamma-activation analysis on a cathode that produced 0.5 MJ of excess heat in a palladium-deuterium experiment performed by Michael McKubre, an electrochemist at SRI International. The analysis showed an 18% reduction of boron-10 in the post-electrolysis cathode compared to its concentration in the virgin material.

**Table 21** Trace elements in electrolyzed and virgin palladium (neutron-activation analysis of Pons' cathode performed at University of Texas, Austin)

<i>Element</i>	<i>Symbol</i>	<i>Electrolyzed Pd</i>	<i>Virgin Pd</i>	<i>Ratio</i>
Cerium	(Ce)	< 5 ppm	< 5 ppm	NA
Cobalt	(Co)	2 ppm	< 0.5 ppm	> 4
Chromium	(Cr)	27 ppm	< 5 ppm	> 5.4
Cesium	(Cs)	14 ppm	< 7 ppm	> 2
Europium	(Eu)	0.04 ppm	0.03 ppm	1.3
Iron	(Fe)	13870 ppm	247 ppm	56
Hafnium	(Hf)	< 0.5 ppm	< 0.4 ppm	NA
Rubidium	(Rb)	< 20 ppm	< 20 ppm	NA
Selenium	(Se)	< 3 ppm	< 3 ppm	NA
Zinc	(Zn)	60 ppm	5 ppm	12

Passell wrote that the "18% depletion in B-10 corresponds almost exactly to the number of reactions of B-10 via the d, alpha reaction to Be-8 needed to explain the 0.56 MJ of excess heat observed."<sup>51</sup>

G.S. Qiao and his colleagues at Tsinghua University, in Beijing, China, observed helium-4 in a palladium-deuterium experiment. But they also analyzed for and found anomalous zinc and terbium, as well as energetic charged particles. They estimated the energy of the charged particles in the MeV range.<sup>52</sup>

George Miley, former director of the Fusion Studies Laboratory at the University of Illinois, Urbana, and former editor of the American Nuclear Society's journal *Fusion Technology*, was one of the few researchers who used both NAA and SIMS to analyze for isotopic shifts.<sup>53</sup> The method gave him qualitative and quantitative data. Miley found 39 elements with isotopic shifts that deviated significantly from natural abundance. Not all species appeared in amounts significantly above detection limits; however, several, such as Fe-56, did.

### Energetic Charged Particles

Energetic charged particles have been observed throughout the history of the field. On occasion, so have low fluxes of neutrons. Both sets of phenomena normally appear in bursts, typically over the course of multi-day experiments, and thus present a challenge to measure. Researchers have also reported calorimetrically measured bursts of excess heat. Future studies may reveal that both bursts take place simultaneously. Electronic detectors have advantages for measuring energetic charged particles, but they average out the signals over time. Therefore, the bursts do not show up in the data. Using solid-state nuclear track detectors (CR-39), however, produces permanent, constantly integrated recordings of nuclear emissions.

The disadvantage of solid-state nuclear track detectors is that the tracks etched into the detectors by particles do not provide a direct measurement of the particle energies or a specific time when the track was made.

In 2002, Andrei Lipson, a physicist at the Institute of Physical Chemistry of the Russian Academy of Sciences, and Alexei Roussetski, a physicist at the Lebedev Physical Institute, used a technique to establish bounds for the energetic particles they observed in a light-water palladium-hydrogen experiment.

"In order to separate high-energy alphas and low-energy protons that could be possibly emitted during electrolysis runs," Lipson and Roussetski wrote, "thin Cu-foils (25-micron thick) were inserted between the cathode metallic coating and the CR-39 surface. 25-micron Cu coating completely absorbs all alpha-particles and protons with energies below 9.0 and 2.3 MeV, respectively. Background measurements in experiments with Cu-covered CR-39 were performed similarly to that with open detectors. As expected, these background experiments showed significant reduction (~2 times) in the total track density compared to that obtained with open CR-39 detectors."

The authors found alpha particles ranging from 11.0 to 16.0 MeV and protons near 1.7 MeV.<sup>54</sup>

One of the more interesting results of particle detection was from an experiment reported in 1998 by Qiao. He and his colleagues observed charged particles emitted from a hydrogen-loaded palladium thin film sandwiched between two CR-39 detectors (Figure 33). After the experiments, they found that the number of etch pits in the area covered by the film was 30 times greater than in the area not covered by the film. In one of the runs, they found a similar pattern on both sets of one pair of detectors. This suggested to the researchers that particles emanated from the foil in both directions. Also, based on the thickness of the film, 1  $\mu$ , the researchers estimated that the energy of the charged particles must be in the MeV range.<sup>52</sup>

### Low-Flux Neutron Emissions

#### Neutrons - India

Neutrons at low intensities have been reported for many years in LENR experiments. A still-unprecedented research effort took place at the Bhabha Atomic Research Centre in Trombay, India, involving 50 scientists in a dozen teams. One of the most significant of those experiments took place on April 21, 1989.

Researchers at BARC performed LENR experiments using a Milton-Roy electrolytic cell. They registered a nearly identical pattern of neutron signals during the experiment, using two independent detectors: a BF<sub>3</sub> counter embedded in paraffin blocks for thermal neutrons, and a proton recoil plastic scintillator counter for fast neutrons. They monitored background signals using 3He counters (Figure 34). Several other groups at BARC also registered neutrons (Figure 35). In addition, several experiments performed at BARC showed instances in which neutrons and tritium were generated at the same time, as well as neutron multiplicity bursts.<sup>55</sup>

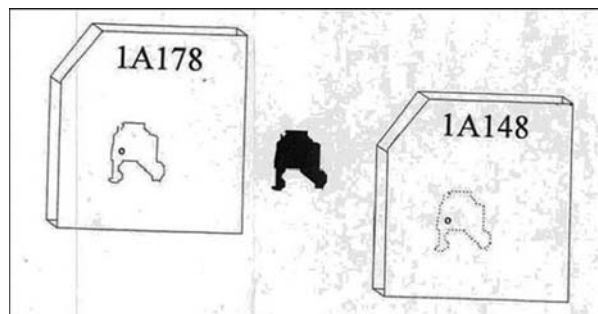


**Figure 33** In the center, palladium thin film is shown adjacent to the two CR-39 detectors that had surrounded it (image courtesy X.Z. Li).

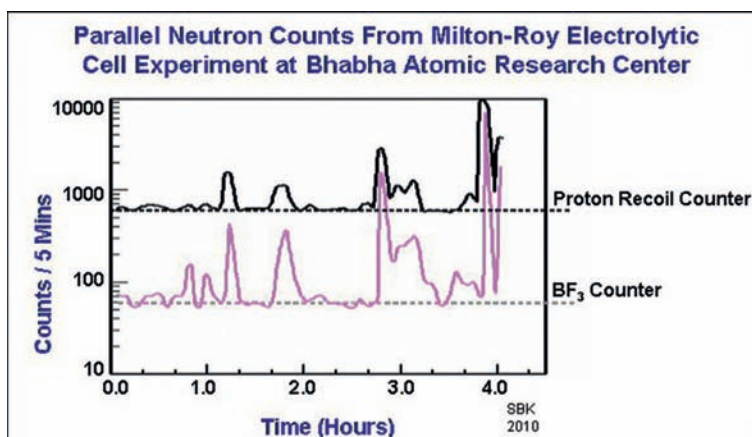


**Figure 34** Neutron counts measured at BARC in LENR experiment.

Summary of Results From Groups Reporting Tritium and Neutrons in BARC Electrolysis Experiments (1989-1990)							
Division	Cathode Material	Shape	Area Cm <sup>2</sup>	Anode	Neutron Yield	Tritium Yield	n / T Ratio
Desalin*	Ti	Rod	104	SS pipe	$3 \times 10^{+7}$	$1.4 \times 10^{+14}$	$2 \times 10^{-7}$
Neut. Phy*	Pd-Ag	Tubes	300	Ni pipe	$4 \times 10^{+7}$	$8 \times 10^{+15}$	$5 \times 10^{-7}$
HWD*	Pd-Ag	Tubes	300	Ni pipe	$9 \times 10^{+7}$	$1.9 \times 10^{+15}$	$5 \times 10^{-7}$
HWD*	Pd-Ag	5 Disks	78	Porous Ni	$5 \times 10^{+4}$	$4 \times 10^{+15}$	$1.2 \times 10^{-8}$
Anal.Ch.@	Pd	Hol. Cyl.	5.9	Pt Mesh	$3 \times 10^{+6}$	$7.2 \times 10^{+13}$	$4 \times 10^{-8}$
ROMg @	Pd	Cube	6.0	Pt Mesh	$1.4 \times 10^{+6}$	$6.7 \times 10^{+11}$	$1.7 \times 10^{-4}$
ROMg @	Pd	Pellet	5.7	Pt Mesh	$3 \times 10^{+6}$	$4 \times 10^{+12}$	$1 \times 10^{-4}$
App.Ch.@	Pd	Ring	18	Pt Mesh	$1.8 \times 10^{+8}$	$1.8 \times 10^{+11}$	$1 \times 10^{-3}$

\* = 5M NaOD Electrolyte @ = 0.1M LiOD Electrolyte SBK 2009

**Figure 35** Tritium and neutron results at BARC.

### Neutrons - USA (SPAWAR)

In March 2007, at the American Physical Society meeting in Denver, Colo., Stanislaw Szpak and Pamela Mosier-Boss, researchers at the U.S. Navy's Space and Naval Warfare Systems (SPAWAR) Center in San Diego, Calif., reported evidence of neutron emission through proton recoil effects observed in electrolytic co-deposition experiments. In the co-deposition process, atoms of palladium (placed into the solution by PdCl) and deuterium (from D<sub>2</sub>O) are deposited, atom by atom, onto a host metal.<sup>56</sup>

The SPAWAR researchers used the CR-39 detectors in two configurations. In the "dry" configuration, they placed the detector just outside the cell, separated by a thin membrane. In the "wet" configuration, they placed a single detector directly in the cell, adjacent to the cathode (Figure 36). In both cases, they also placed control detectors in the vicinity, to analyze for background particles. For cathodes, they used a substrate consisting of Pt, Ag or Au. They placed the palladium chloride into the electrolytic solution containing deuterium. After the palladium plated out onto the substrate, they observed evidence of charged and neutral particles.

Initially, the researchers were looking only for evidence of energetic charged particles on the sides of the detectors facing the cathodes. However, they also discovered tracks on the sides of the detectors facing away from the cathodes. The researchers realized that alpha particles could not go through the full thickness of the detector, and they determined that such tracks were from neutrons. For charged particles to traverse through the 1 mm CR-39 plastic, 40 MeV particles would have been required, and apparatus to produce such particles were not present in the SPAWAR environment.

The tracks on the back side of the detectors faced away from and had no contact with the cathodes. In at least one experiment, three parallel wires against a CR-39 detector produced parallel sets of tracks on the front as well some tracks on the back side of the detector. The sets of tracks on the front were spatially correlated with the cathode, and one set of tracks on the back was spatially correlated with the Pt wire. The researchers reported a very strong signal-to-noise ratio (Figures 37 and 38).

This experimental protocol appears to be one of the few relatively inexpensive experiments that, according to SPAWAR researchers, are fully repeatable. They found evidence of energetic charged alpha particles in each experimental run. Although the researchers did not search for excess heat at the same time, the same protocol produced excess heat in the previous set of experiments.<sup>57</sup>

### Neutrons - USA (SRI International)

In 2009, researchers at SRI International replicated the SPAWAR experiment and, using a BF<sub>3</sub> detector, observed apparent neutron counts above background in at least three experiments.

In one of these experiments (Figure 39), SRI International researcher Francis Tanzella reported a measurement of a neutron burst 14 times higher than background, which ran for 14 h. Concurrently with the onset of the neutron signal, Tanzella observed a distinct drop in cell potential, suggesting a heating effect in the electrolyte. The cell was not instrumented for calorimetry.<sup>58</sup>

SRI International also used several CR-39 detectors in this experiment. One detector also showed a neutron signal when it was independently analyzed in Russia by yet a third method, serial etching, by Roussetski and Lipson. They confirmed that the detector showed "real nuclear (proton recoil) tracks." Additionally, they compared the signals to a known neutron source and concluded that the "experimental evidence can be considered as a strong, unambiguous proof of fast neutron (2.5 MeV) exposure" (Figure 40).

The SRI International detector analyzed at the Russian Academy of Sciences was transported internationally along with a control detector, and because the control detector did not show significant tracks, the researchers concluded that the detectors were not irradiated by airport security.

### Neutrons - Italy

In November 2012, LENR researcher Domenico Cirillo reported at the American Nuclear Society meeting in San Diego, Calif., another experimental configuration to detect neutrons.<sup>59</sup>

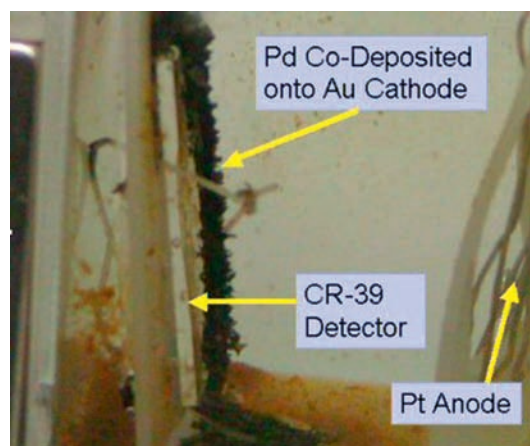


**Figure 36** Pd co-deposited onto cathode wire in SPAWAR LENR experiment.

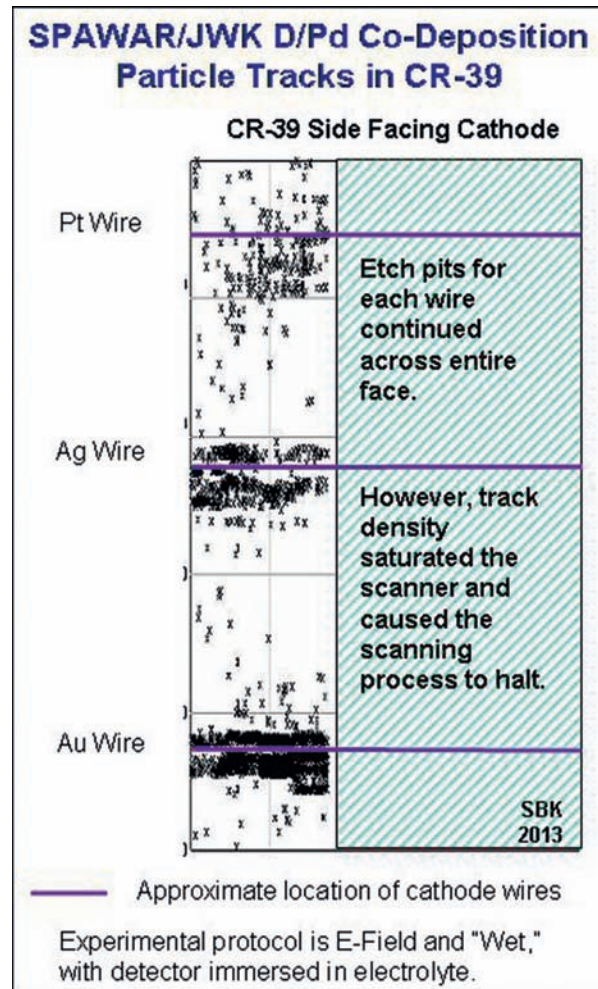


**Figure 37** Computer scan of solid-state nuclear track detector (CR-39) showing tracks from three cathode wires facing CR-39.

Cirillo works with the plasma electrolytic LENR system with light water. He developed a novel method using solid-state nuclear track detectors (CR-39) to show evidence for low-intensity neutron emissions from LENR experiments.

He uses a small hermetically sealed polystyrene cylinder into which he places the CR-39 detector, and he fills it with boric acid grains (Figure 41). He places the cylinder into the solution, in the vicinity of the tungsten cathode. The boron acts as a neutron absorber. Alpha particles cannot travel the distance from the cathode and through all the materials to reach the CR-39 detector, but neutrons, which can easily reach the boron within the cylinder, convert into alpha particles and, when emitted, create particle tracks on the CR-39.

His CR-39 calibrations have been confirmed with a reference neutron flux generated by an Am-Be neutron source by the Italian National Institute for Ionizing Radiation Metrology, part of the Italian National Agency for New Technologies, Energy and Sustainable Economic Development in Casaccia, Italy. Cirillo reported that "a significant number of tracks were recorded by the CR-39 detectors exposed to the plasma discharge, while the corresponding blank samples did not reveal any relevant activity."

The detected neutrons would not be expected to correlate quantitatively either with observed heat production or production of ultra-low-momentum neutrons. ULM neutrons do not generally have enough energy to leave the immediate vicinity of the nano- to micron-scale reaction site. The emitted and detected neutrons may also be the result of spallation neutrons, caused by ULM neutrons. Cirillo also wrote that his thermal neutron flux measurements have relatively low efficiency." Cirillo wrote:

This is because of the sequence of events required to produce a track on the CR-39 detector: Neutrons must be emitted into the detector at a solid angle, then they have to meet a boron-10 nucleus contained in the boric acid grains (boron-10 is only 18.7 % among the total boron contained in  $H_3BO_3$ ), then the alpha particles must be emitted into the detector at a solid angle, reach the detector sample without being absorbed by the converter material, and finally they must hit the detector leaving a new track in a sample area free of previous ones.



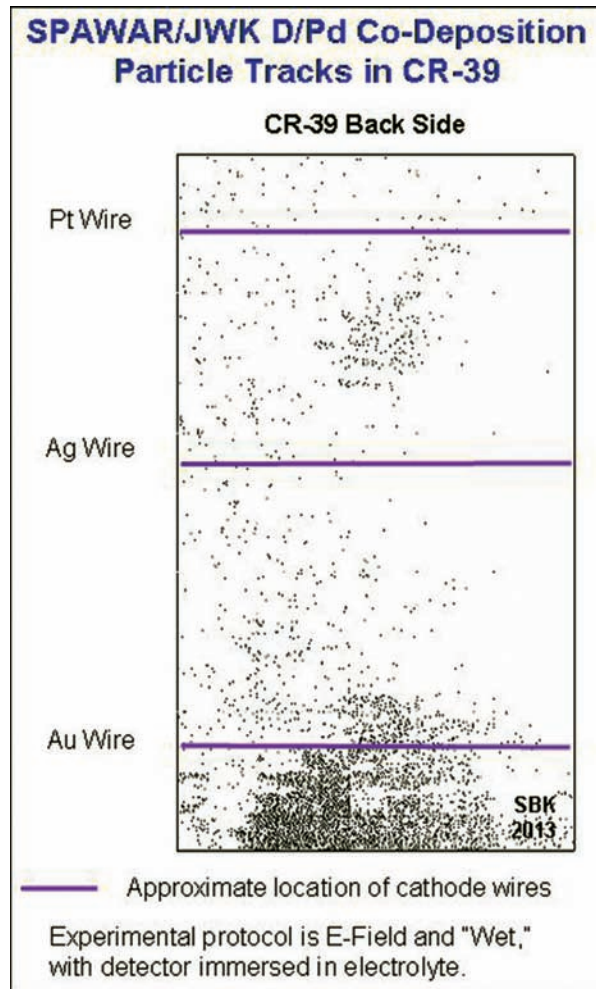


**Figure 38** Computer scan of solid-state nuclear track detector (CR-39) showing tracks on back side of same CR-39 detector.

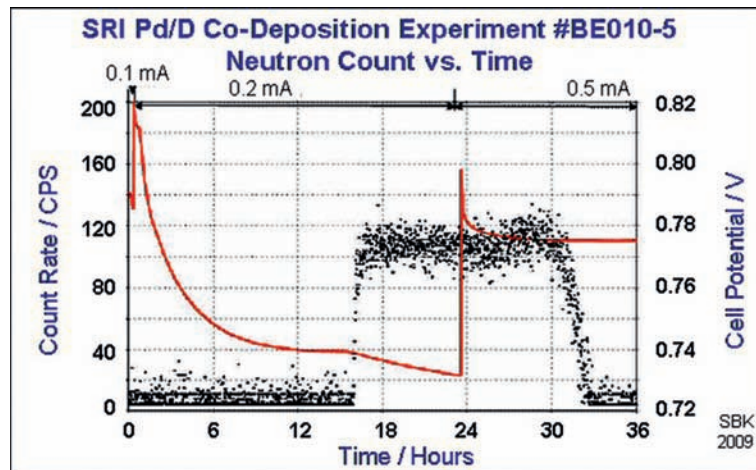


**Figure 39** SRI International's replication of SPAWAR co-deposition experiment. Neutron signal is  $14 \times$  greater than background during 14-hour burst. Measurement by  $\text{BF}_3$  ionizing neutron detector placed about 10 cm from operating cell. The drop in cell potential is temporally correlated with the onset of neutron signal and suggests cell heating.

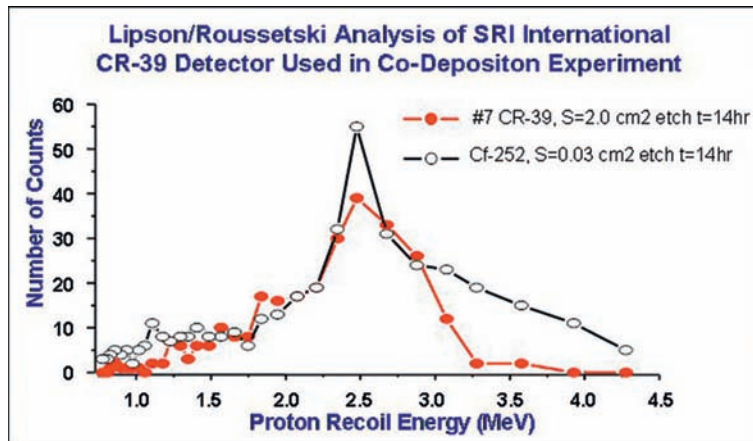


**Figure 40** Comparison of proton recoil from known neutron source to emissions from Pd/D co-deposition experiment.



**Figure 41** Polystyrene cylinder contains CR-39 detector surrounded by boric acid (images courtesy D. Cirillo).

## Light-Element Transmutations

### *Tritium and helium-3*

One of the most distinctive nuclear products of LENRs is tritium. Tritium decays rapidly; it has a half-life of 12.3 years. For this reason, the source of any tritium found above background, must be a man-made event.

It is not seen often in LENRs, but it has been observed at scientifically significant levels. Helium-3 has also been measured, and this may be a direct product of LENRs or a secondary product of tritium decay. In electrolytic experiments, tritium has been measured both in the gas phase and in the electrode.

One of the first teams to observe tritium evolution from a LENR experiment was Padmanabha Krishnagopala Iyengar and Mahadeva Srinivasan at the Bhabha Atomic Research Centre (BARC), in Trombay, India.<sup>60</sup> The BARC researchers witnessed a burst on April 21, 1989, and reported it to the scientific community in July 1989. In December 1989, the government of India published their research and that of 19 other groups at the laboratory in the book *BARC Studies in Cold Fusion: Report 1500*. The BARC researchers found tritium in palladium-deuterium systems and later in nickel-hydrogen systems.

At Texas A&M University, a group led by John O'Mara Bockris noticed extremely high concentrations of tritium in its experiments on April 24, 1989.<sup>61</sup>

The paper reported that 11 out of a set of 24 cells produced tritium at levels "100 to  $10^{15}$  times above that expected from the normal isotopic enrichment of electrolysis."

The Bockris group sought and obtained extensive confirmations of the tritium after the initial analysis at Texas A&M. Additional analyses were performed by Los Alamos National Laboratory (National Tritium Center), Argonne National Laboratory, Battelle Pacific Northwest Laboratory, and General Motors Research Laboratory.

An experiment performed at SRI International, repeating one designed and originally performed at Osaka University by Arata and Zhang, produced tritium and helium-3.<sup>24</sup>

The key part of the Arata-Zhang cell design was the cathode: a hollowed-out 14 mm rod of palladium. Inside the cavity, researchers placed finely divided palladium, also called palladium-black, then welded the top closed before the experiment began. Normal electrolysis took place on the outside of the cathode. However, when deuterium dissociated from D<sub>2</sub>O in the electrolyte, it passed into and through the Pd walls and entered the inner chamber.

Arata-Zhang found helium-4 in that experiment. In their Arata-Zhang replication, SRI found no helium-4 but reported total production of tritium between  $2 \times 10^{15}$  and  $5 \times 10^{15}$  atoms.<sup>62,63</sup>

After the experiment, the cylindrical cathode was sectioned horizontally, and an assay was performed on the radial section for helium-3 on the inside of the chamber, on the outer wall of the chamber, and at five intermediate locations between the two.

Helium-3 was found at all points, the highest from inside the chamber, then sequentially lower at each of the remaining six locations. These data support the claim that the helium-3 or tritium was created inside the chamber. Decay rates from the tritium indicate that the causative event occurred during cathodic electrolysis (Figure 42).

A group led by Thomas Claytor at Los Alamos National Laboratory found tritium, as well, as did other groups (Figure 43).<sup>64,65</sup>

**Helium-4**

At least half a dozen reports show the production of helium-4. Typically, researchers also observe the production of excess heat at the same time helium-4 is produced.

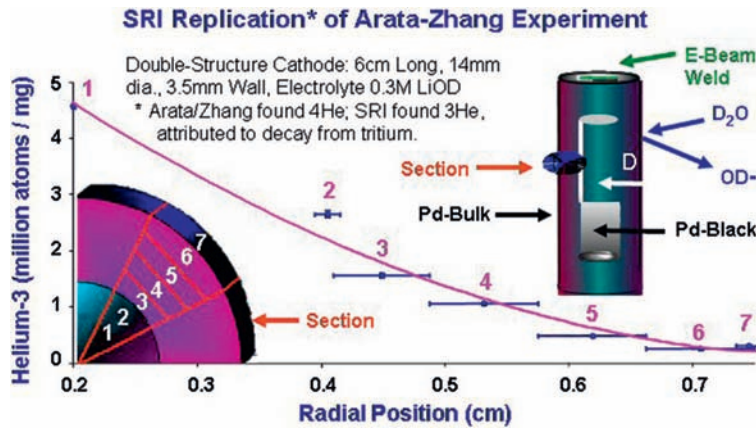


Figure 42 Helium-3, attributed to decay from tritium, found in higher concentrations on the inside of the cathode.

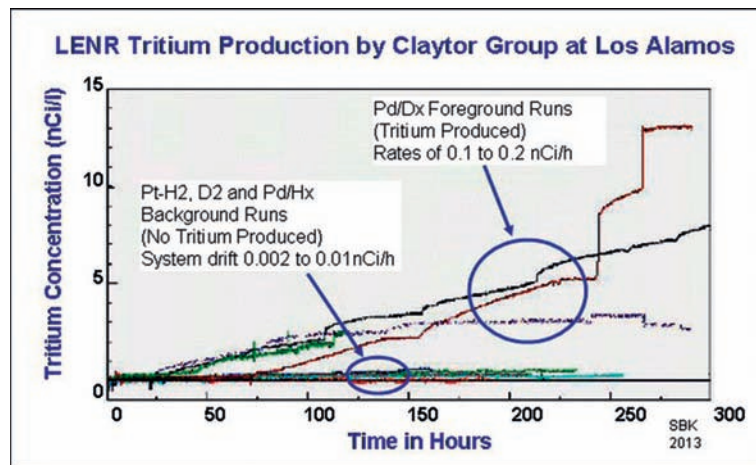
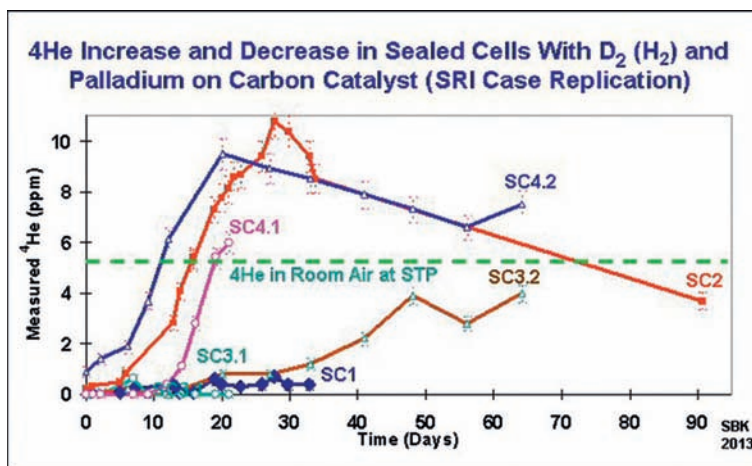


Figure 43 Tritium generation rates up to 25 times larger than control experiments.



**Figure 44** Increase and decrease of helium-4 in palladium-on-carbon/deuterium(hydrogen) gas cell.

Helium-4 can be difficult to distinguish from deuterium without the use of a high-resolution mass spectrometer. Another issue makes helium a difficult nuclear ash to identify and measure: It readily permeates many materials, including glass.

In the early 1990s, electrochemist Melvin Miles was at the U.S. Navy's China Lake facility, working with analysts Ben Bush and J. Joseph Lagowski from the University of Texas, Austin. Miles was one of the first researchers to find helium-4 in LENR experiments. However, his first experiments were performed in glass cells. Critics, citing the normal presence of helium-4 in the air, rejected Miles' initial claim. Miles and, independently, Bockris at Texas A&M University subsequently performed experiments in stainless steel and detected significant amounts of helium-4.<sup>66,67</sup>

One of the clearest helium-4 results was obtained in an experiment at SRI International when researchers repeated an experiment developed by Les Case, a researcher in New Hampshire, using a palladium catalyst.<sup>68</sup>

The SRI researchers wrote that "experiments in ... which Pd on C catalyst materials were exposed to D<sub>2</sub> and H<sub>2</sub> gases for prolonged periods, exhibited a range of behaviors." The researchers displayed a graph which they said contained "6 of 16 results obtained in paired cells." Their graph went up to 48 h. One of the researchers, McKubre, provided *New Energy Times* with complete data for the six runs, which went out to 95 h (Figure 44).

Air from the active cells as well as control cells was evacuated before starting the experiments. All cells showed a starting value of helium-4 close to zero. The SRI researchers failed to label which runs were made with deuterium and which were made with hydrogen. Three runs, (SC4.1, SC4.2 and SC2), presumed to be deuterium, showed a rapid rise of helium, exceeding the level of room air helium.

The decreases in helium-4 for runs SC2, SC4.2 and SC3.2 have at least two possible explanations. The SRI International researchers ruled out the possibility that the vessel was leaking. They proposed that ad- or absorption in palladium and/or carbon (carbon was a key material used in the experiment) was taking place.

Larsen, however, proposed that a nucleosynthetic reaction cycle could have started using the helium-4 as a reactant and thus began consuming it. When cells SC4.2 and SC3.2 began to rise again, Larsen speculated that a new helium-4 production cycle had started.<sup>69</sup>

## Heavy-Element Transmutations

### *Miley's Nickel-hydrogen electrolysis experiments*

Heavy-element transmutations were first reported in the early 1990s largely through the work of Bockris at Texas A&M University.

In 2003, Miley conducted a survey, "Review of Transmutation Reactions in Solids" and found that heavy-element transmutations had been reported by 15 independent laboratories.<sup>70</sup>

In the mid-1990s, Miley performed a series of experiments with nickel and hydrogen. In one of these sets, he performed six runs, then charted the abundance of various product elements by mass number. He noticed a distinct five-peak spectrum, which Larsen later recognized as a function of the creation and capture of ultra-low-momentum neutrons. Miley speculated on a different mechanism for the unique spectrum (Figure 45).<sup>20</sup>

### *Mizuno's Palladium-deuterium electrolysis experiments*

Also in the late 1990s, at Hokkaido University, in Japan, Mizuno was working with the palladium-deuterium system. He too saw a similar but not identical multippeak pattern of atomic abundances. Miley's peak curve is based on data from multiple runs; Mizuno's data in this graph (Figure 46) is based on the analysis of only one run. The groupings for Miley and Mizuno are slightly different, and this reflects the difference in starting seed materials and neutron production.<sup>71</sup>

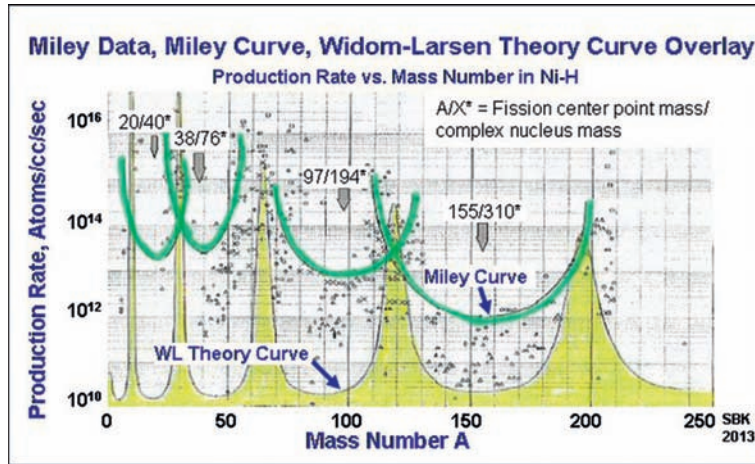


**Figure 45** Miley-Widom/Larsen correspondence - Upper 5-peak curve drawn by Miley in 1996 based on 6 experimental runs of transmutation yields from Ni-H LENR systems. Lower curve, shaded in yellow, drawn by Larsen in 2006 with no fitting, based on Widom-Larsen ultra-low momentum neutron absorption model.<sup>9,29</sup>

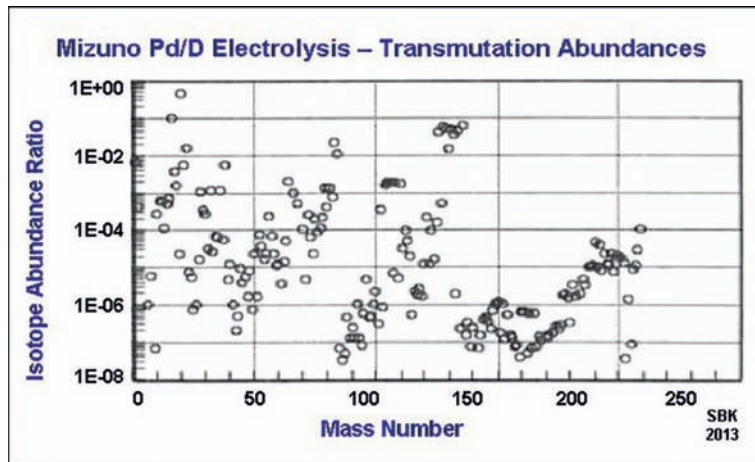


**Figure 46** Mizuno's transmutation abundances.

### ***Miley-Mizuno-Widom/Larsen's correspondence***

The Miley work, done with the Ni/H system, and the Mizuno work, done with the D/Pd system, both show the distinctive five-peak spectrum. The Widom-Larsen theory explains the distinct spectrum.

The qualitative predictions of the Widom-Larsen optical model include:

- five-peak product-mass spectrum from  $A = 1$  to  $A = 250$
- peaks approximately at atomic mass numbers 12, 31, 62, 117 and 206
- position of each of the peaks in terms of mass number ( $A$ )
- increased spacing between successive peaks as  $A$  increases
- declining amplitude of peaks as  $A$  increases

Widom and Larsen do not claim that the optical model would necessarily have a quantitative high  $r^2$  coefficient of correlation between model output and any arbitrary collection of experimental data points. This is because significant amounts of statistical noise are randomly introduced in such limited amounts of data from complex LENR nucleosynthetic network processes operating in significantly different types of experiments that are run over variable lengths of time (Figure 47).

Where Mizuno identified a range for the peaks he observed, they equate to mass numbers 65, 120 and 194. Where Miley identified a range for the peaks he observed, they equate to mass numbers 25, 65, 120 and 200. Widom and Larsen calculated the transmutation peaks, based on their theoretical model, to occur around mass numbers 12, 31, 62, 117 and 206 (Table 22).

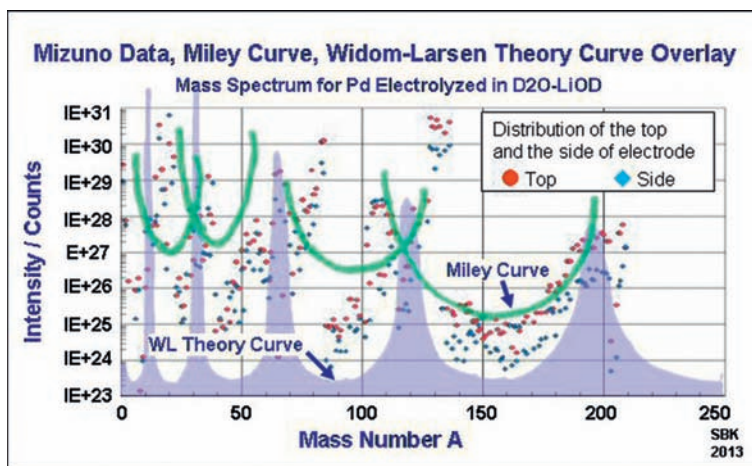


**Figure 47** Mizuno-Miley-Widom/Larsen correspondence: Data points (in blue and red) are plotted by Mizuno. Upper 5-peak green curve is an overlay from Miley experiment, drawn by Miley for his data in 1996.<sup>29</sup> Lower curve, shaded in purple, drawn by Larsen in 2006 with no fitting, based on Widom-Larsen ultra-low momentum neutron absorption model.<sup>9</sup> Mass spectrum of SIMS measurement for Pd sample surface, which generated excess heat, after electrolysis in 1991. Confirmatory tests also with EDX, AES, EPMA, ICP-MASS. Two areas of surface were analyzed and show similar spectra.<sup>48</sup>

**Table 22** Mizuno – Miley – Widom-Larsen theory correspondences: Mass peaks of LENR transmutation abundances

	Peak 1	Peak 2	Peak 3	Peak 4	Peak 5
Mizuno <sup>71</sup>			65	120	194
Miley <sup>20</sup>		25	65	120	200
WLT <sup>72</sup>	12	31	62	117	206

### Iwamura's Gas-permeation experiments

A well-measured series of LENR transmutation experiments has been performed by Iwamura and co-workers at Mitsubishi Heavy Industries in Japan for more than a decade. The experiment causes deuterium gas to pass through a multilayered substrate containing palladium and calcium oxide. On the front side of the substrate, atoms from the new element are found in place of the element initially deposited there. Through gas pressure and a low-power heater alone, they cause the simultaneous gradual increase of a target element and the gradual decrease of a starting (given) element. Iwamura reported a positive correlation between deuterium gas permeation and the elemental conversion rate. The Mitsubishi researchers have repeated this type of observation many times, with several pairs of elements. If similar reactions are occurring with hydrogen permeation, they are taking place below the detection limits (Figures 48 and 49).<sup>35</sup>

The gradual increase of one element and the temporally correlated gradual decrease of another element have occurred in all of their experiments, making the conjecture of simultaneous gradual contamination (of target elements) and gradual redistribution (of given elements) by some skeptics extraordinarily unlikely. The Iwamura process is patented in Japan. In Figure 11, the Mitsubishi XPS data show similar patterns among three sets of experimental runs (Figure 50).

The Mitsubishi group has confirmed its LENR transmutations by a variety of methods, including TOF-SIMS, XANES, X-ray fluorescence spectrometry and ICP-MS. Some of the analyses have been performed *in situ*, and some have been performed at the Japanese Spring-8 Synchrotron. The resultant elements also often show anomalous isotopic ratios.

A group led by Miyamaru Higashiyama, at Osaka University, was the first to report a replication of the cesium-to-praseodymium reaction. The group did so in each of three runs. Akira Kitamura, at Kobe University, reported a replication of the barium-to-samarium reaction, and Francesco Celani, at the Italian National Institute of Nuclear Physics in Frascati, reported a replication of the strontium-to-molybdenum reaction using electrolysis. In 2012, a group from Toyota Central Labs also reported a partial replication.

This experiment is quite costly; however, it appears to be one of the few experiments that, according to Iwamura, have given him positive results every time (Figure 51).

According to Iwamura, Mitsubishi is considering his research for three potential applications. The first is for a transmutation facility for radioactive cesium. Mitsubishi is a manufacturer of fission reactors, and cesium-137 is a normal byproduct. The second application is the production of rare metals, such as platinum, from abundant metals, such as tungsten. The third application is electrical power generation from excess heat.

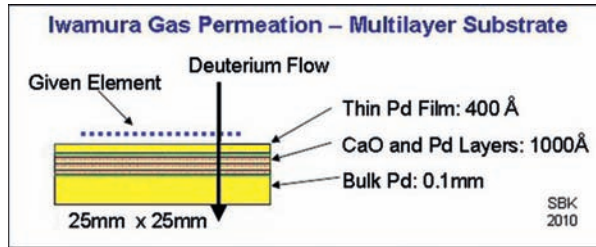


Figure 48 Mitsubishi Heavy Industries/Iwamura Multilayer Substrate.<sup>73</sup>

### Iwamura Transmutations Summary

133 55	Cs	M+8 Z+4	→	141 59	Pr
88 38	Sr	M+8 Z+4	→	96 42	Mo
138 56	Ba	M+12 Z+6	→	150 62	Sm
137 56	Ba	M+12 Z+6	→	149 62	Sm
44 20	Ca	M+4 Z+2	→	48 22	Ti
184 74	W	M+4 Z+2	→	188 76	Os

MITSUBISHI DATA      SBK 2012

Figure 49 Some of the reported Mitsubishi LENR transmutations.

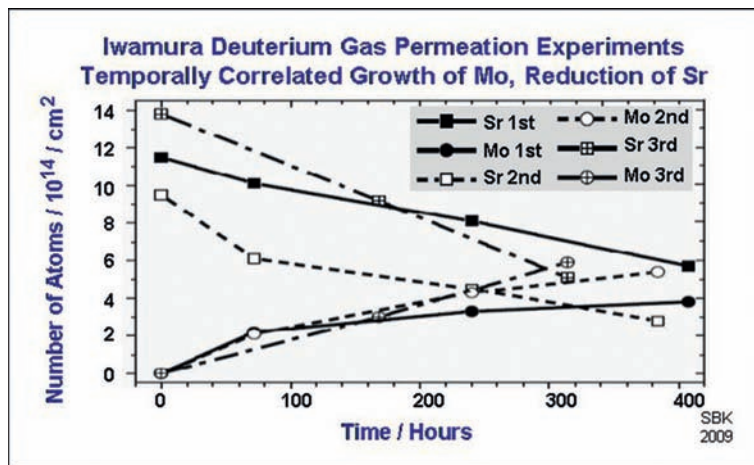
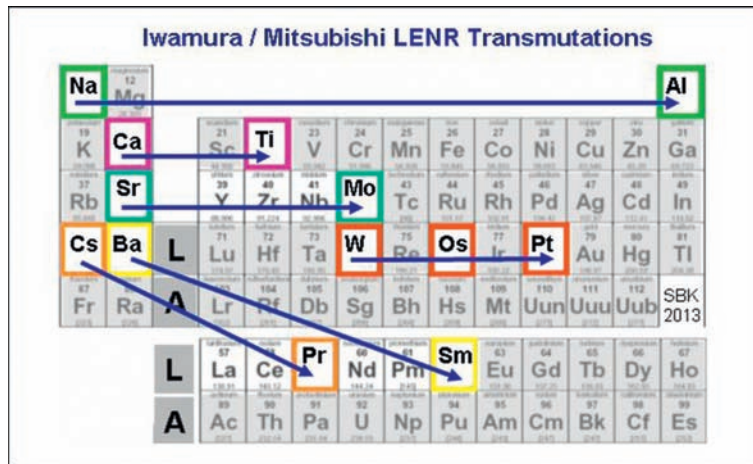
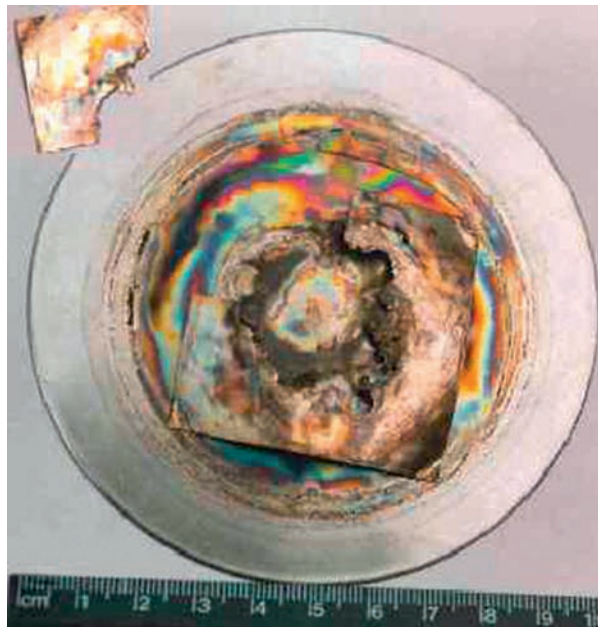


Figure 50 Temporally correlated gradual decrease and increase of elements.



**Figure 51** MHI LENR transmutations: Na to Al, Ca to Ti, Sr to Mo, Cs to Pr, Ba to Sm and W to Os or Pt.



**Figure 52** Two pieces of metal: a  $50 \times 50 \times 0.01$  mm Pd foil in front of a 40 mil thick 10 cm stainless steel disk. The pieces were used together by Stringham during a 20-hour acoustic cavitation experiment. The colored pattern on the stainless steel disk is caused by the migration of Pd atoms to the disk. The thin layer of Pd or palladium oxide deposits on the stainless steel disk and the condition of the melted Pd foil indicate very high transient and local temperatures sufficient to vaporize Pd. This experiment was performed around 1994–1995. (Photo courtesy: R. Stringham).

## Surface Anomalies and Morphological Changes

### *Vaporized metal*

In 1989, when LENR researcher Roger Stringham heard of the Fleischmann–Pons experiment, he applied his experience using acoustic cavitation in photochemical synthesis and pioneered a new method of LENR experiments. To Stringham, acoustic cavitation seemed just as viable a method for loading deuterium into materials as the electrochemical method used by Fleischmann and Pons.

Stringham's method uses ultrasonic waves to stimulate LENRs within closed cells. It is distinct from acoustic inertially confined fusion. Acoustic inertially confined fusion does not use condensed matter inside the apparatus, and its proponents claim that it yields the expected byproducts of thermonuclear fusion.

Stringham has produced evidence of melted and even vaporized 100- $\mu$ m target foils as a result of his LENR acoustic cavitation experiments.

The acoustic energy inputs varied from 5 to 16 W, with exposures of 5 min to several weeks in duration (Figure 52).

Scanning electron microscope (SEM) photomicrographs of the foils after the experiments show a palladium surface that looks identical to melted metal, as well as nanometer-size-diameter eruptions that he calls ejecta sites.



None of these effects can be caused by Joule heating or by arcing because this type of experiment involves no electrolysis; only acoustic energy is input to these experiments.

### Hot spots

LENR researchers have observed a variety of surface anomalies and morphological changes to cathodes used in LENR experiments. The anomalies include morphological deformations, craters, and “hot spots.” While the LENR group at SPAWAR was active between 1989 and 2012, it produced some of the most interesting experiments and observations in the field and published more LENR papers in mainstream journals than any U.S. LENR group.

In one of the most creative experiments, the SPAWAR researchers aimed an infrared video camera at an active cathode during the experiment. The camera was oriented perpendicularly to the cathode. They explained the configuration in their slide presentation.

“This experimental set up is an example of the flexibility that co-deposition provides. In this case, we co-deposited onto a Ni mesh that was physically placed close to a mylar film, covering a hole in the cell wall,” the researchers wrote. “An IR camera was positioned to focus on the electrode, and recordings were made during and after the co-deposition process to monitor the temperature of the electrode and the surrounding solution. These tests were conducted with the help of professor [Massoud] Simnad, from UCSD, and Dr. Todd Evans, from [General Atomics] Inc., who provided the IR camera.”

(Video Courtesy SPAWAR): <https://www.youtube.com/watch?v=OUVmOQXBS68>. Video of infrared video camera aimed at cathode during LENR co-deposition experiment at SPAWAR.

The experiment was instructive in three ways. First, the thermal imaging showed that the cathode does not heat up with a uniform thermal gradient across the entire material. Instead, it shows that the heat comes from many tiny spots on the cathode. This information supports other experimental data, including anomalous isotopic distributions and anomalous morphological changes that take place on the surface, also in discrete, localized spots.

Second, because the researchers used a video camera rather than a still camera, it becomes clear that these hot spots are born and die in microseconds.

According to Larsen, these spots are in fact patches of even smaller units in the micron-scale LENR-active environment that have a lifespan of no more than 300 ns.

Larsen describes them as contiguous many-body monolayer patches of collectively oscillating protons on a surface that, combined with surface plasmon electrons, is oscillating and entangled collectively.<sup>74</sup>

The images below are sequential frames from the thermal video taken by SPAWAR at a rate of 32 frames per second. The first set (Figures 53–55) is taken at 19:44:53, and the second set (Figures 56–58) is taken at 19:46:07. The SPAWAR researchers wrote that the nuclear active site must contain a large number of single events to produce a visible image. The spots in white indicate temperatures that were above and beyond the range of the camera.

The third piece of information, while not surprising, was still supportive; it showed that the cathode, rather than Joule heating, was the heat source (Figure 59). The thermal gradient from the center to the edge of the cathode is the inverse of the gradient that would occur if caused by Joule heating. The thermal gradient from the center to the perimeter of the cathode is visible in the infrared images above.

The SPAWAR researchers also used a piezoelectric transducer in the cell, which was both temperature- and pressure-sensitive, as they explained in 2003 (Figure 60).

“The flashes observed in the IR experiments suggest ‘mini-explosions,’ so we designed an experimental setup to see if we could record these events using a piezoelectric sensor,” the researchers wrote. “Again, the co-deposition approach made this possible. A piezoelectric transducer was coated with epoxy as an insulation layer except for approximately 1 cm<sup>2</sup> on the front, on which an electrically conducting material (Ag) was deposited. This became the cathode onto which Pd was co-deposited from the PdCl in a deuterated water solution.”

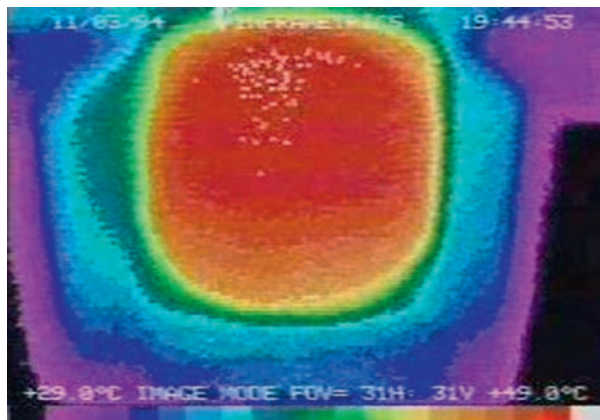


**Figure 53** Frame 1 from first set of sequential frames from SPAWAR thermal imaging video.

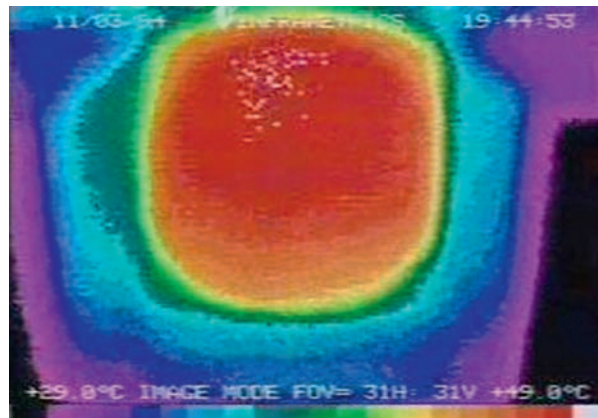


**Figure 54** Frame 2 from first set of sequential frames from SPAWAR thermal imaging video.

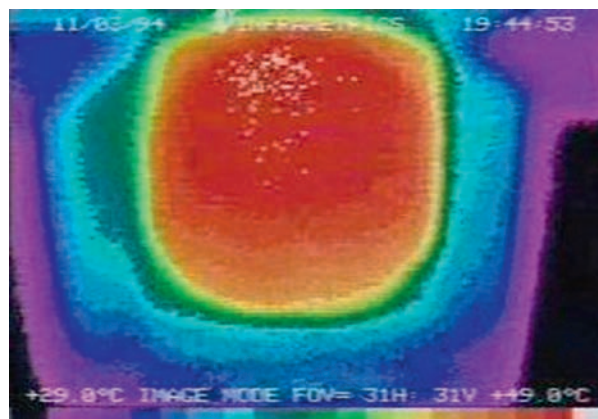


**Figure 55** Frame 3 from first set of sequential frames from SPAWAR thermal imaging video.

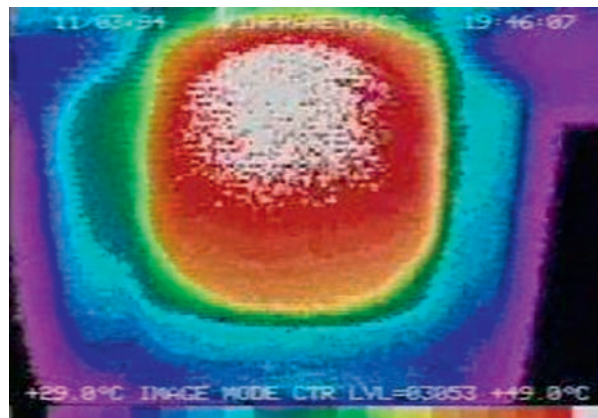


**Figure 56** Frame 1 from second set of sequential frames from SPAWAR thermal imaging video.

In the same way that the infrared video displayed small, discreet events, the transducers also picked up discrete temperature and pressure spikes, which the SPAWAR researchers identify as mini-explosions. This kind of instrumentation offers the possibility of real-time feedback on when the events occur, as well as their flux. The researchers explained the features of the transducer in 2003.

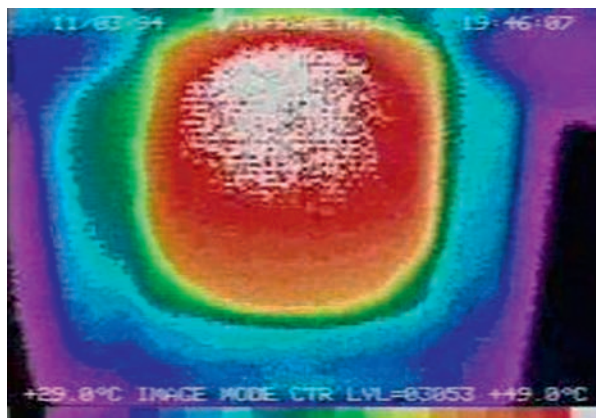


Figure 57 Frame 2 from second set of sequential frames from SPAWAR thermal imaging video.

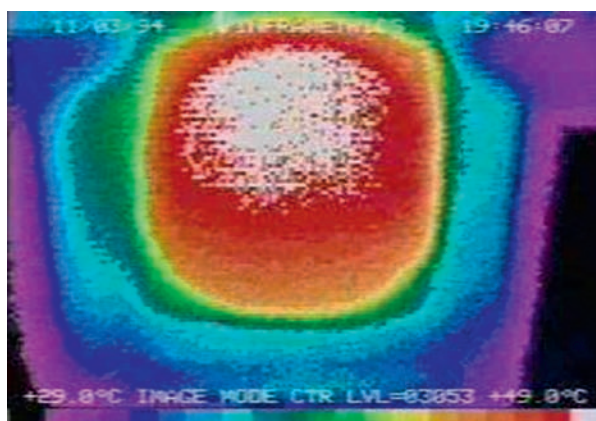


Figure 58 Frame 3 from second set of sequential frames from SPAWAR thermal imaging video.

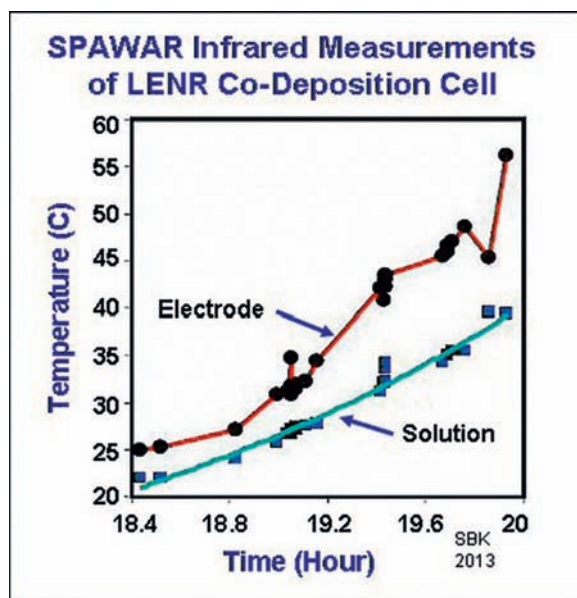
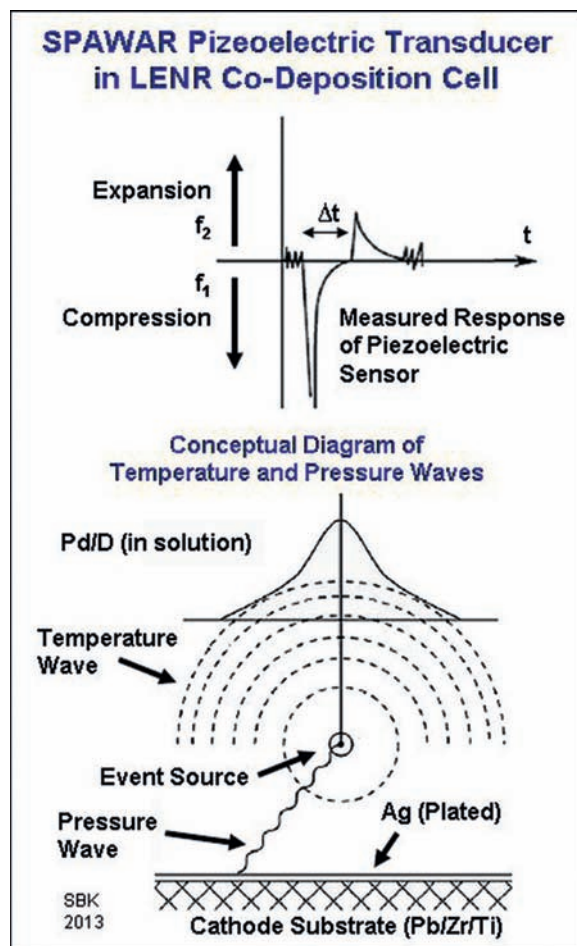


Figure 59 SPAWAR temperature comparison between electrode and electrolytic solution.



**Figure 60** Diagram showing signal response from piezoelectric transducer.

“The sharp spike down is a result of compression on the sensor, and the swing above the line is caused by expansion,” the researchers wrote. “These signals are representative of an initial pressure wave impinging on the sensor, which causes compression, followed by a localized increase in temperature, which causes expansion. The diagram suggests an explanation which is consistent with the observed measurements. The pressure wave propagates at the speed of sound through the metal. Heat propagation is much slower. It’s also worthwhile to note that these observed responses continued after the current to the cell was turned off, which is consistent with ‘heat after death’ reports that others have seen. Although it was observed that the frequency and intensity of the events decayed with time, a few events were still observed after 3 days.”<sup>75</sup>

### **Morphological changes**

Many researchers have observed a variety of unusual morphological changes (Figures 61–75) to the surfaces of the cathodes.

Researchers at the Proton-21 Electrodynamics Laboratory, based in Kiev, Ukraine, experiment with a unique method in which an electron beam is directed to a metal target (typically a wire) that is placed in the center of a disk, which they call an accumulating screen (Figures 76–78). The beam energy, directed to the target from the outside, causes the target to be destroyed by an explosion from the inside. The explosion causes dispersion of the target material, which is precipitated onto the accumulating screen. The group has reported a variety of phenomena resulting from these experiments, including transmutation of heavy elements and creation of superheavy elements. They have also performed experiments using radioactive material for targets and have found a decrease in gamma radiation afterward.<sup>40</sup>

Between 1999 and 2000, the group performed 6000 experimental runs, which they called dynamic compressions of solid targets. They performed 15 000 analyses of 800 samples using a variety of methods, including X-ray electron probe microanalysis, auger-electron spectroscopy, mass-spectrometry and Rutherford backscattering.

Even though the Proton-21 protocol does not include an explicit step to load hydrogen into the metal, and the experiments take place in a vacuum, the researchers found the presence of anomalous hydrogen and deuterium in post-experiment analyses, which is required for LENR reactions.

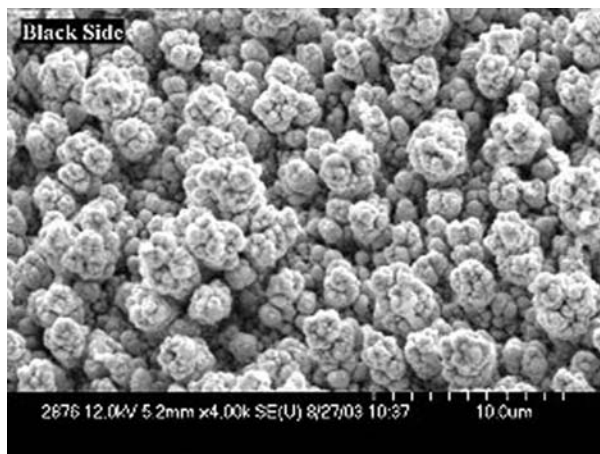


**Figure 61** Normal surface morphology from control experiment (SPAWAR).<sup>76</sup>

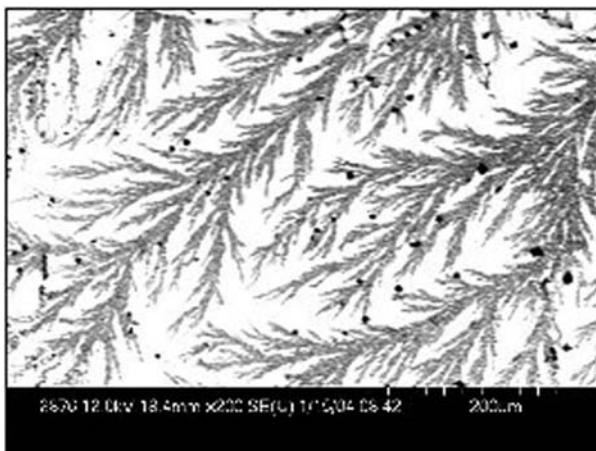


**Figure 62** Morphological changes after experiment: fractals (SPAWAR).

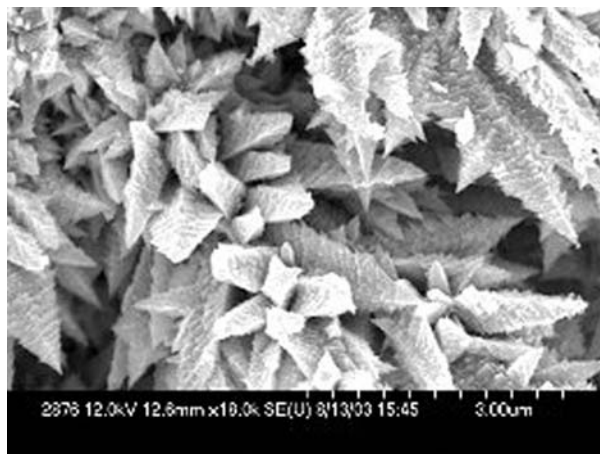


**Figure 63** Morphological changes after experiment: Dendritic Growth (SPAWAR).



**Figure 64** Morphological changes after experiment: Long Wires (SPAWAR).

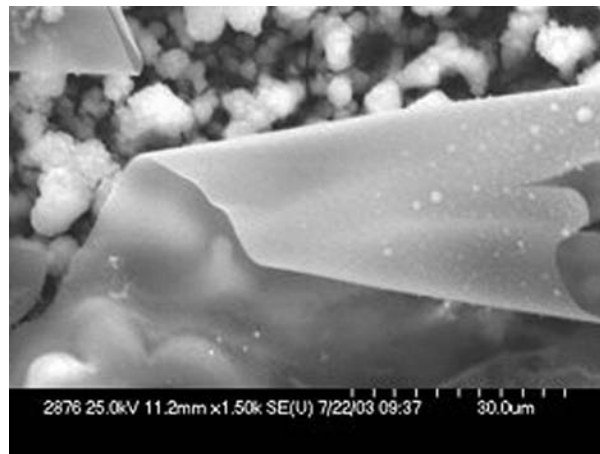


**Figure 65** Morphological changes after experiment: Folded Thin Films (SPAWAR).

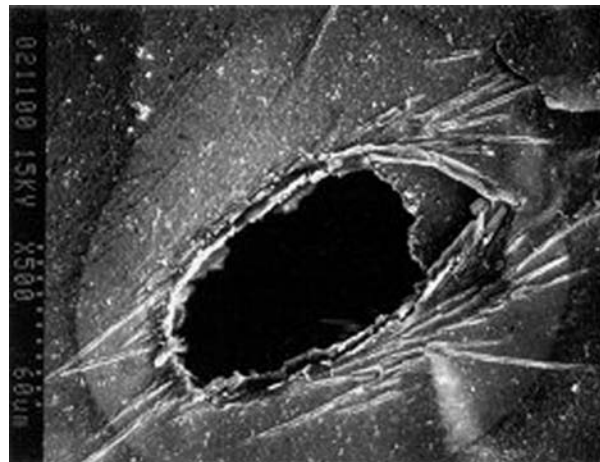


**Figure 66** Morphological changes after experiment: Craters (SPAWAR).

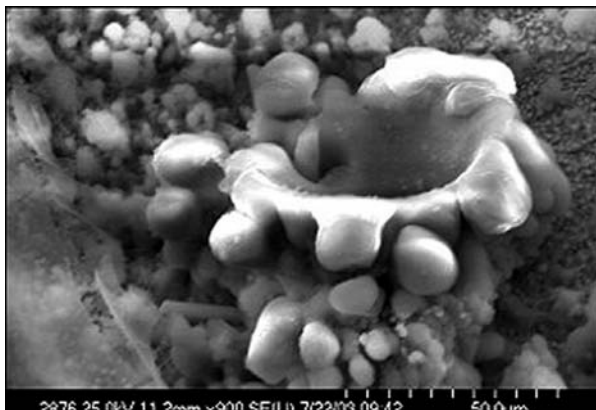


**Figure 67** Morphological changes after experiment: SEM image of molten Pd on Au foil used as a cathode in a 2003 SPAWAR electrolytic co-deposition experiment with an external electric field (6000 V). Sample resembles molten metal that has cooled quickly. This suggests that a high-temperature event occurred, followed by fast cooling from immersion in electrolyte. Photo: Charlie Young.

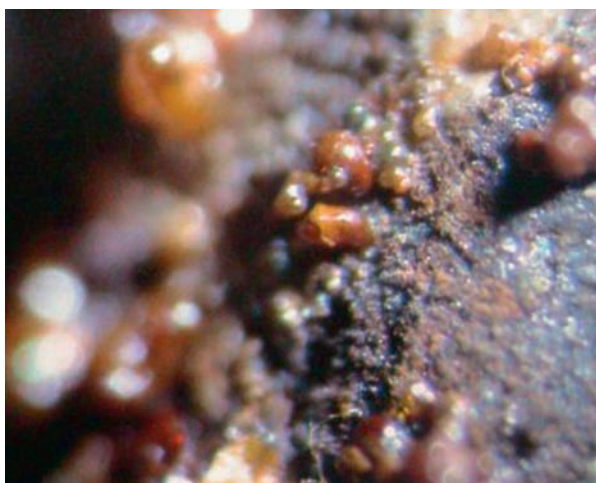


**Figure 68** Ni alloy rod nearly melted and recrystallized from Piantelli experiment. Optical microscope photo taken by Piantelli after eight-month experimental run. Peak thermally measured power in the system:  $99.5 \text{ W} \pm 2 \text{ W}$  (28.5 W power in, 71 W excess heat).

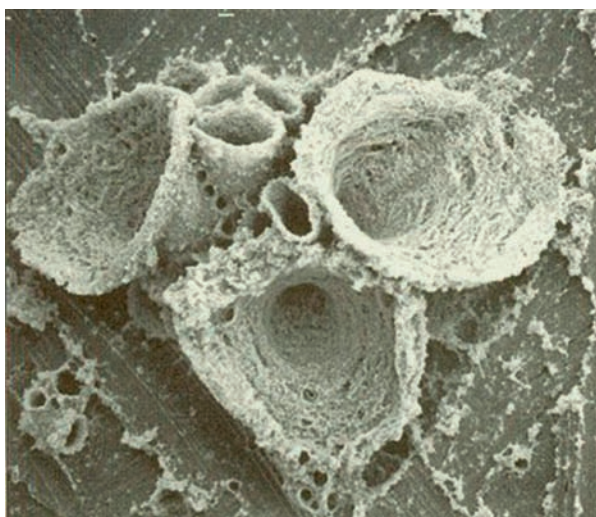


**Figure 69** Protrusions and cones observed on the surface of gold cathode after electrolysis (Tadayoshi Ohmori and Tadahiko Mizuno). The cones are about  $10 \mu\text{m}$  in diameter and  $15 \mu\text{m}$  high. Ohmori described the structure of the cones as a fine mesh, and he found not only gold but also platinum, iron and other elements.<sup>77</sup>

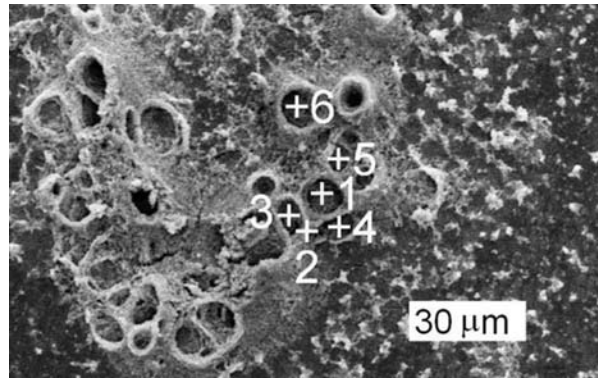


**Figure 70** SEM image of portion of cathode after electrolysis LENR experiment performed at Portland State University by Dash and colleagues. They found localized, high concentrations of anomalous silver in the newly formed craters. Locations mark areas where they analyzed for elemental concentration.<sup>21</sup>

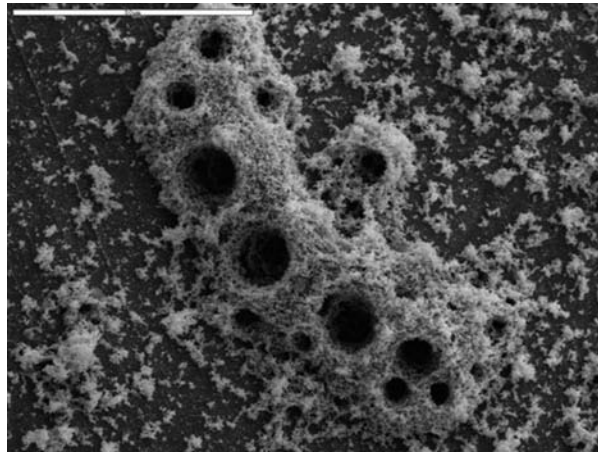


**Figure 71** Volcano-like structures seen in SEM picture of electrode surface at 1000 magnification after electrolytic experiment performed by Mathieu Valat at Portland State University in 2010. The scale bar is 50  $\mu\text{m}$  long.<sup>78</sup>

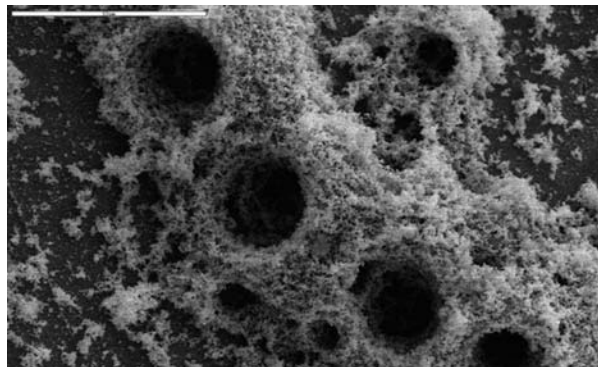


**Figure 72** Close-up of volcano-like structures at 1000 magnification.



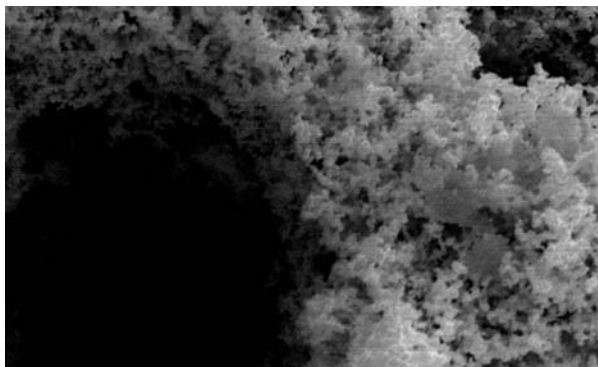


**Figure 73** Close-up of volcano-like structure at 5000 magnification.

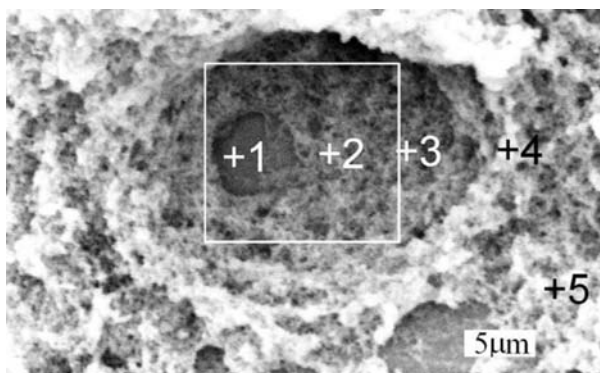


**Figure 74** Dash found that the silver concentration varies by a factor of five from spots within the craters versus spots on the outside of craters. The relative atomic percent concentrations of  $\text{Ag}/(\text{Pd} + \text{Ag})$  in the entire area shown above was  $1.2 \pm 0.5$ . The area within the white square was  $5.6 \pm 0.4$ . Spots 1–5 were 5.6, 6.3, 3.6,  $1.2 \pm 0.4$ , respectively.<sup>21</sup>

6.8, 5.6, 6.3, 3.6, 1.2

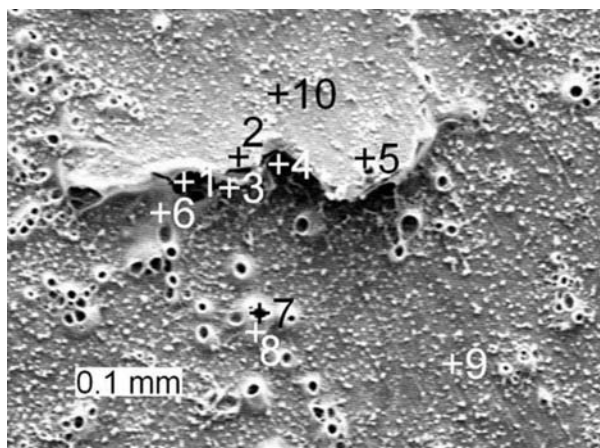


**Figure 75** Another view of craters on a post-experimental cathode by Dash. Dash analyzed for and found anomalous concentrations of silver.<sup>21</sup>

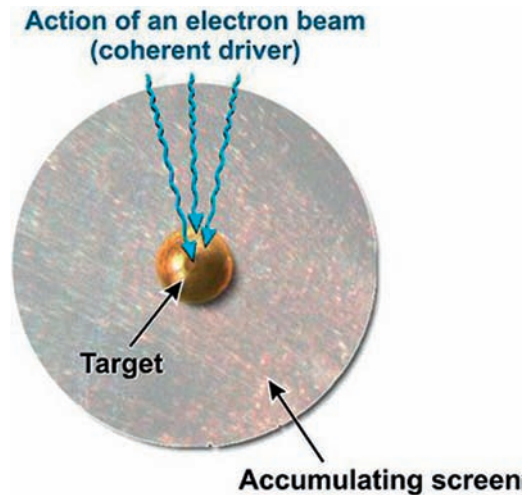


**Figure 76** Diagram showing accumulating screen and target. (Courtesy Proton 21).

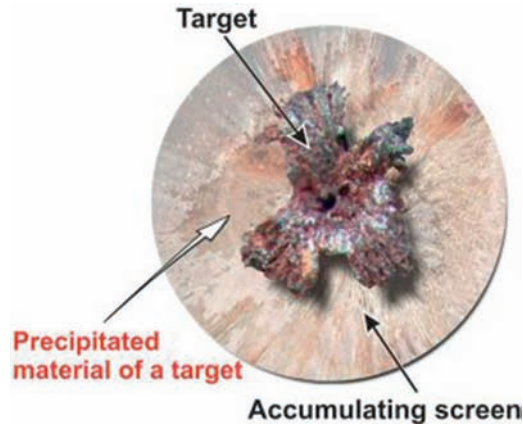


**Figure 77** Diagram showing accumulating screen and remains of target. (Courtesy Proton 21).



**Figure 78** Photos of copper target before and after beam compression. (Courtesy Proton 21).

Below are some of the photographs (Figures 79–82) of the metallic targets and screens after the electron beam-induced compressions. The analyses for elemental composition are performed on the accumulation screens as well on the ejected substances. The text overlays on the photos display the concentrations of various chemical elements in specific locations of the screens and/or the remains of the targets. The researchers made a particular point of highlighting (in yellow) elements that were absent in the composition of the starting materials.

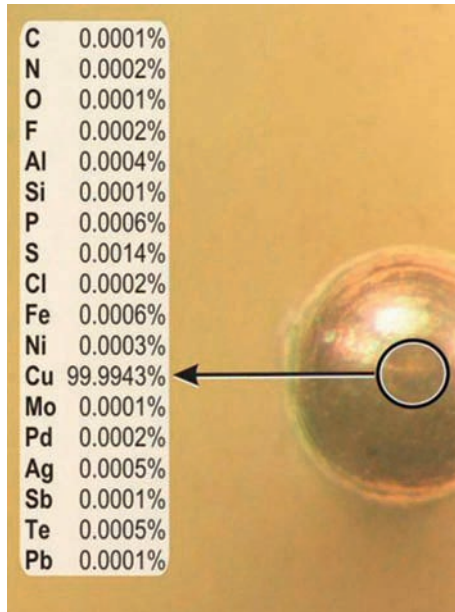


**Figure 79** Proton-21 target before experiment. Target material is copper (Cu 99.99%). The method of investigation is glow-discharge mass-spectrometry. Analyzed mass range is up to 250.

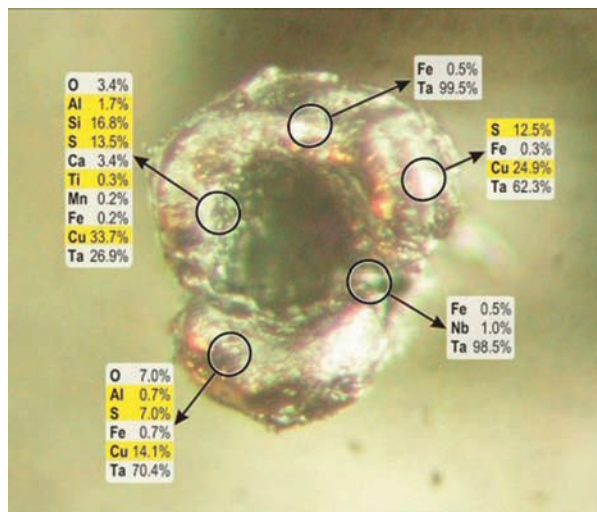


**Figure 80** Proton-21 target after experiment No. 1754. Target material is tantalum (Ta 99.68%). The method of investigation is X-ray electron probe microanalysis. Element detection range is from B to U.

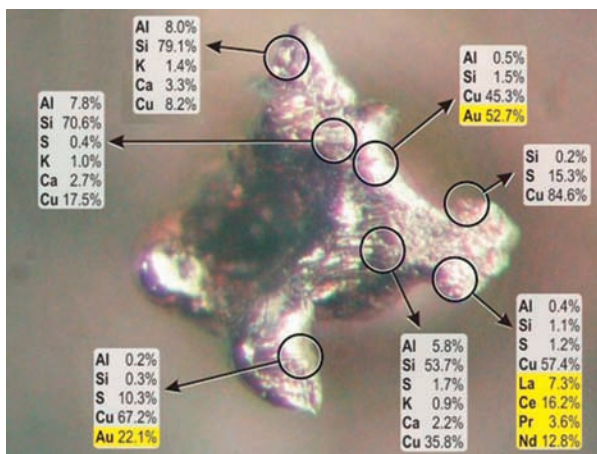


**Figure 81** Proton-21 target after experiment No. 2107. Target material is copper (Cu 99.99%). The method of investigation is X-ray electron probe microanalysis. Element detection range is from Na to U.

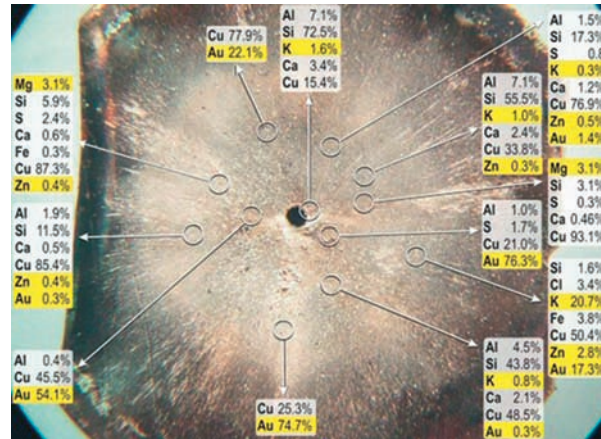


**Figure 82** Proton-21 accumulating screen after experiment No. 2107. The material of the accumulating screen is copper (Cu 99.99%). The method of investigation is X-ray electron probe microanalysis. Element detection range is from Na to U.

## Excess Heat and Calorimetry

### Excess Heat

When LENR experiments produce more heat than the electrical energy put into them, this is called excess heat. Two common methods that researchers use to produce excess heat are D/Pd electrolysis, in general replicating Fleischmann and Pons, and Ni-H gas loading. Examples of both methods are given below.

#### *Palladium-deuterium electrolytic system - IMRA*

After Fleischmann and Pons left the National Cold Fusion Institute, on the campus of the University of Utah, they went to work in the Toyota-sponsored laboratory Institut Minoru de Recherche Avancée in Nice, France. Few LENR researchers have achieved the magnitude of excess heat that they did while they were in the IMRA lab. In what may be perhaps Pons' last paper from the work at that lab, he lists two colleagues as co-authors, T. Roulette and Jeanne Roulette, but not Fleischmann. This suggests that Pons and Fleischmann had stopped working together by that time.

Roulette, Roulette and Pons reported seven runs in the series of experiments; two of them were exemplary (Table 23). Run #3 produced 101 W of excess heat for 30 days, giving 294 MJ of excess energy. Run #4 produced 17 W of excess heat for 70 days, giving 102 MJ of excess energy.<sup>19</sup>

#### *Palladium-deuterium electrolytic system - SRI International*

Researchers performed a set of experiments at SRI International in 2006–07 as part of a joint project with Energetics Technologies LLC, the University of Rome and the Italian National Agency for New Technologies, Energy and the Environment in Frascati. They did not operate their experiments at temperatures as high as the ones run by Pons in 1995, and this may explain the lower levels of excess heat. Of 23 experiments, 14 produced excess heat, primarily in the milliwatt range (Table 24).

#### *Nickel-hydrogen gas-loading and electrolytic systems*

Many nickel-hydrogen LENR research studies were performed, mostly in the 1990s. An excellent review of this work is provided in a 1998 paper by Giuliano Mengoli and his colleagues.<sup>79</sup>

One of the most significant sets of Ni-H research was performed by a group led by Piantelli, a biophysicist when he was in the Department of Physics at the University of Siena, and Sergio Focardi, in the Department of Physics at the University of Bologna, in the 1990s. Their group presented and published a dozen papers on the topic. Whereas electrolytic D/Pd experiments have typically produced scientifically meaningful levels of excess heat, such effects were typically observed only in the milliwatt range. The Piantelli group's Ni-H gas experiments produced excess heat in the tens of watts.

The Piantelli group used hydrogen gas in combination with nickel rods inserted into a stainless steel chamber (Figure 83).

The experimental configuration is relatively simple. A small stainless steel cylinder about the size of a beverage can contains a nickel rod 5 mm in diameter by 90 mm long. Also inside the cylinder is an electrical resistance heater - in concept, much like a coil that is used to heat a cup of coffee or a blanket. Air is pumped out of the cylinder, then hydrogen is gradually introduced. Initially, some of the hydrogen is absorbed, or loaded, into the nickel, and this occurs over the course of several cycles. Once the hydrogen is fully loaded into the nickel, the reactions begin to take place.

In 2008, *New Energy Times* published a detailed description and photo-essay of the experiment in the article "Deuterium and Palladium Not Required."<sup>80</sup>

**Table 23** Summary of 7 experiments performed at IMRA Europe

Experiment	1	2	3	4	5	6	7
Cathode	Pd	Pd	Pd	Pd	Pd	Pd	Pd
Rod size, mm	100x2	100x2	100x2	100x2	100x2	12.5x2	12.5x2
Anode	Pt coil	Pt coil	Pt coil	Pt coil	Pt coil	Pt mesh	Pt mesh
Electrolyte:0.1 M	LiOD	LiOD	LiOD	LiOD	LiOD	LiOD	LiOD
Electrolyte, mL:	90.7	90.0	90.6	97.0	97.0	90.4	90.9
Expt time, days	94	134	158	123	123	47	60
$P_{\text{w excess}}/W/4.2 \text{ hr}$	-0.1	-0.6	101	17.3	13.8	74.5	39.4
Total energy, MJ	-0.0	-5.5	294	102	0.3	30.5	-7.6
% excess power	0	0	150 (30d)	250 (70d)	0	Variable	~0

**Table 24** Excess-heat experiments performed at SRI International in 2006–07 (partial listing)

Calorimeter			Mm. R/R	Max. D/Pd	Maximum excess power		Total excess energy, (kJ)
Cell	Site	Cathode			% of power in	mW	
43–7	S	L14-2	1.73	0.903	80%	1250	245
43–8	S	ETI	1.63	0.923	5%	525	05
43–9	S	L14-3	1.61	0.927	1%		
51–7	S	L25B-1	1.55	0.939	12%	266	176
51–8	S	L25A-2	1.52	0.945	5%	133	14
51–9	S	L19	1.54	0.941	43%	79	28
56–7	S	L24F	1.55	0.939	15%	2095	536
56–8	S	L24D	1.84	0.877	4%		
56–9	S	L25B-2	1.56	0.937	3%		
57–8	S	Pd-C	N.A.	N.A.	300%	93	115
58–9	S	L25A	1.69	0.911	200%	540	485
61–7	S	L25B-1	1.63	0.923	50%	105	146

The full list of experiments includes four runs with power in excess of 1 W. Excess power, as a percentage of power input, ranges from around 5% to 300%.

**Figure 83** Piantelli Ni-H cell, in center, attached to gas manifolds and thermocouples.

They published several experiments, reporting 18 and 72 W of excess heat – 600 and 900 MJ of energy integrated – over 319 and 278 days, respectively. They also reported evidence of neutrons, gamma rays, charged particles, and the presence of anomalous elements.

Their 1994 *Il Nuovo Cimento* paper was challenged by E. Cerron-Zeballos and co-workers from CERN in 1996. The Piantelli group published a successful rebuttal in 1998.<sup>12</sup> In 2008, *New Energy Times* published a detailed analysis of the debate in the article “Piantelli-Focardi Publication and Replication Path.”<sup>81</sup>

The following table (Table 25) displays a summary of the group’s work.<sup>14</sup>

**Table 25** Summary of Piantelli group's Ni-H LENR work

Lab (Group) Ashes	Start	Sample	Hydrogen Loading	Days	Excess heat (W)	Excess Energy(MJ)
Siena (1) $\gamma$ -ray: No; Neutrons: No; Altered metal surface: Yes	Jan. 1992	Ni cylinder	High	36	12	Not valued
Siena (2) $\gamma$ -ray: No; Neutrons: No; Altered metal surface: Yes	Oct. 1993	Ni-plated Ni-alloy cylinder	High	55	44	>90
Siena (3) $\gamma$ -ray: Yes; Neutrons: Yes; Altered metal surface: Yes	Sept. 1994	Ni-plated Ni-alloy cylinder	Very high	278	72	~900
Siena (3) $\gamma$ -ray: Yes; Neutrons: No; Altered metal surface: No	Nov. 1994	Ni-plated Ni-alloy cylinder	High	319	18	~600
Siena (3) $\gamma$ -ray: Yes; Neutrons: No; Altered metal surface: Yes	March 1996	Ni-plane	Medium	22	27	38
Siena $\gamma$ -ray: Yes; Neutrons: No; Altered metal surface: Yes	July 1996	Ni-plane	Very low	0	0	0
Bologna (4) $\gamma$ -ray: No; Neutrons: No; Altered metal surface: Yes	June 1996	Ni-alloy cylinder	High	n/a	n/a	Not valued
Colleferro (5) $\gamma$ -ray: No; Neutrons: No; Altered metal surface: Not analyzed	Sept. 1997	Ni-alloy cylinder	Medium	147	8	~100
Siena (3) $\gamma$ -ray: Yes; Neutrons: No; Altered metal surface: No	Nov. 1997	Ni plane	Low	0	0	0
Pavia (6) $\gamma$ -ray: No; Neutrons: No; Altered metal surface: Not analyzed	Sept. 2001	Ni-plated Ni-alloy cylinder	Medium	n/a	n/a	Not valued

*Researchers:* 1. Piantelli; 2. Focardi, Habel, Piantelli; 3. Focardi, Gabbani, Montalbano, Piantelli, Veronesi; 4. Campari, Focardi, Gabbani, Montalbano, Piantelli, Veronesi; 5. Focardi, Gabbani, Montalbano, Piantelli, Porcu, Tosti, Veronesi; 6. Focardi, Cattaneo, Gabbani, Montalbano, Nosenzo, Piantelli, Piazzoli, Veronesi.

## Calorimetry

Excess heat is measured in LENR experiments using calorimetry, a science that goes back 200 years. The purpose of calorimetry is to measure the heat that comes from an experiment.

Calorimetry involves the use of mechanical devices as well as precise calculations. However, modern methods use calibrated electrical measurements.

In general, LENR researchers use any (or some combinations) of three types of calorimeters: isoperibolic, mass-flow, and enclosure (Seebeck-type) calorimeters. Some researchers who claimed to find no excess heat with light hydrogen may have made an unstated assumption that light hydrogen does not produce excess heat. For example, McKubre wrote that, in one of his gas experiments, "the calorimetry was performed in a relative (rather than absolute) manner so that the excess heat measured in the D2 gas cell was the excess over that in the H2 cell (which was presumed to be zero) as a blank."<sup>82</sup>

Relative, or differential, calorimetry is important to understand because a) some researchers reported examples of excess heat in heavy-hydrogen experiments by comparing them to light-hydrogen experiments and this may have understated excess heat in both cases. The first person to report a slight signal of excess heat in light-water LENRs was no other than Pons, in a press conference at the American Chemical Society meeting in Dallas, Texas, on April 12, 1989.

**Figure 84** shows a simple electrolytic cell used by John Dash and his students at Portland State University. **Figure 85** is a schematic of the cell drawn by a master's candidate, Mathieu Valat, while at Portland State University.

### Isoperibolic calorimetry

Several variations of isoperibolic calorimeters exist. In the simplest configuration, the cell is immersed in a constant temperature bath, and two sensors measure the temperature, one inside the cell and another outside the cell in the water bath. The rate of heat transfer can then be measured.

Other isoperibolic calorimeters surround the cell with an insulating layer that provides additional thermal isolation of the cell from the water bath. In these calorimeters, the temperature within this insulating layer, called the thermal barrier, is measured in addition to or in place of the temperature directly within the cell.

Isoperibolic calorimetry was the preferred choice for Fleischmann and Pons (**Figure 86**), though people who were not experts in calorimetry were concerned that its complexity could give rise to sources of error. Isoperibolic calorimetry is not intrinsically complex; however, it becomes so when a mixture of radiative, conductive, and convective heat flows must be accounted for. The distrust of isoperibolic calorimetry by non-experts caused many electrochemists to move to mass-flow calorimetry in an attempt to satisfy the intense and understandable skepticism of the non-experts toward LENR excess heat.

Mathieu Valat, while performing LENR research for his master's degree in physics at Portland State University, analyzed for excess heat and isotopic changes. Valat used isoperibolic calorimetry, with temperature sensors at different locations inside the cell. His temperature curves show fairly typical and moderate excess-heat rises in the experimental cell (**Figure 87**) over a period of time, while the curves for the control cell (**Figure 88**) stay flat. Valat also found anomalous shifts in palladium isotopes after the



**Figure 84** Simple electrolytic cell used by students at Portland State University. During experiment, cathode foil begins to curve and approach anode.

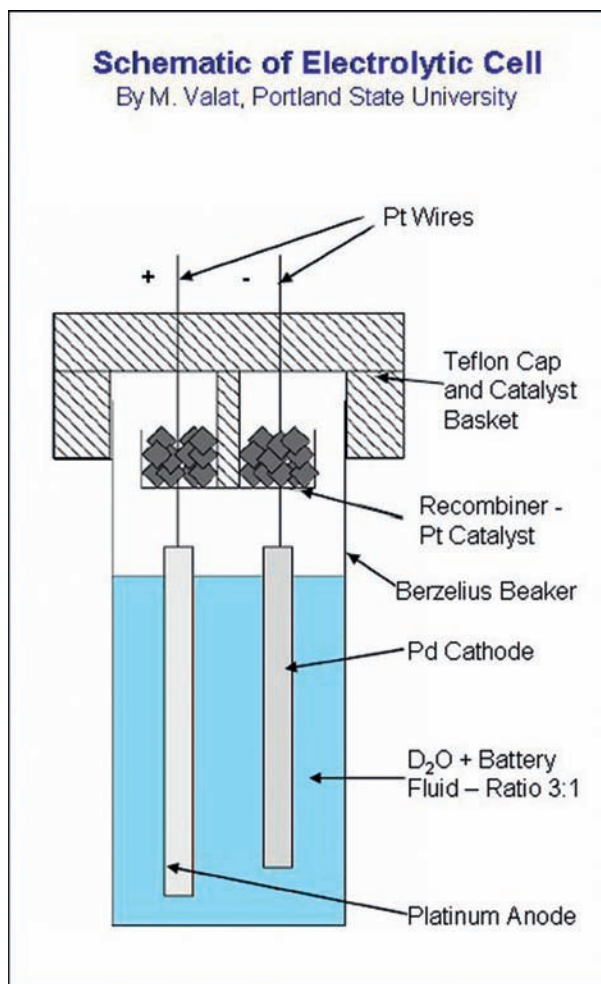


**Figure 85** Schematic of simple electrolytic cell drawn by Mathieu Valat at Portland State University.

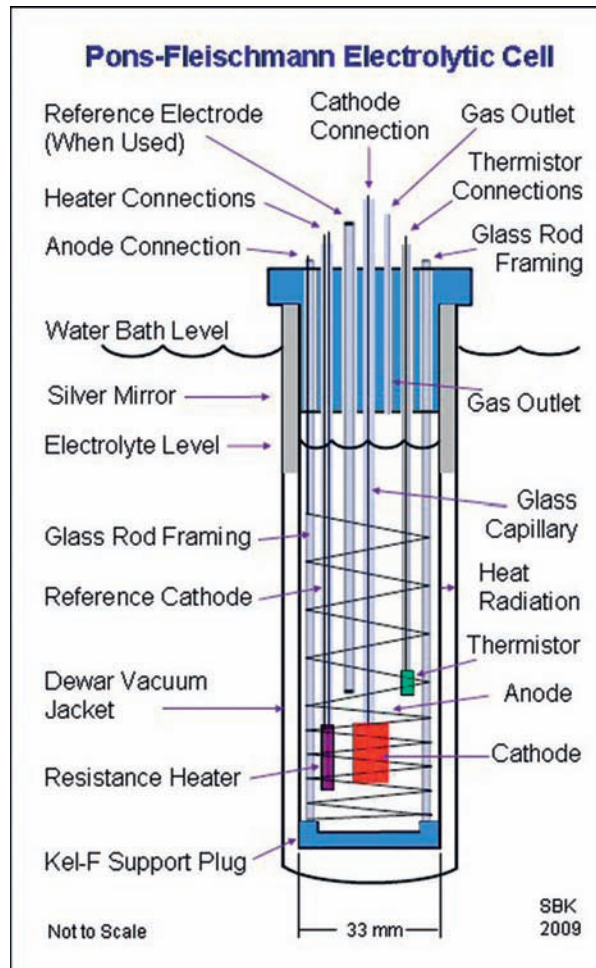


**Figure 86** Diagram of Fleischmann-Pons electrolytic cell using isoperibolic calorimetry.

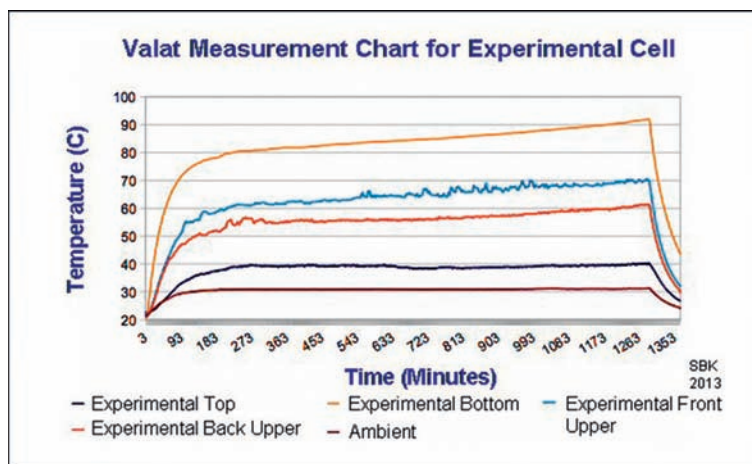


**Figure 87** Valat measurement chart for experimental cell shows continuous temperature rise after the first 200 min. Cell ran in parallel with control cell, both at constant current. Voltage varies based on resistance changes in electrolyte.



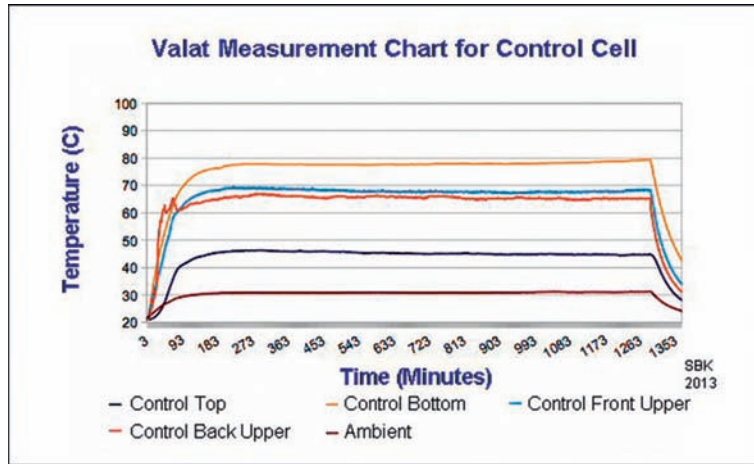


**Figure 88** Valat measurement chart for control cell.

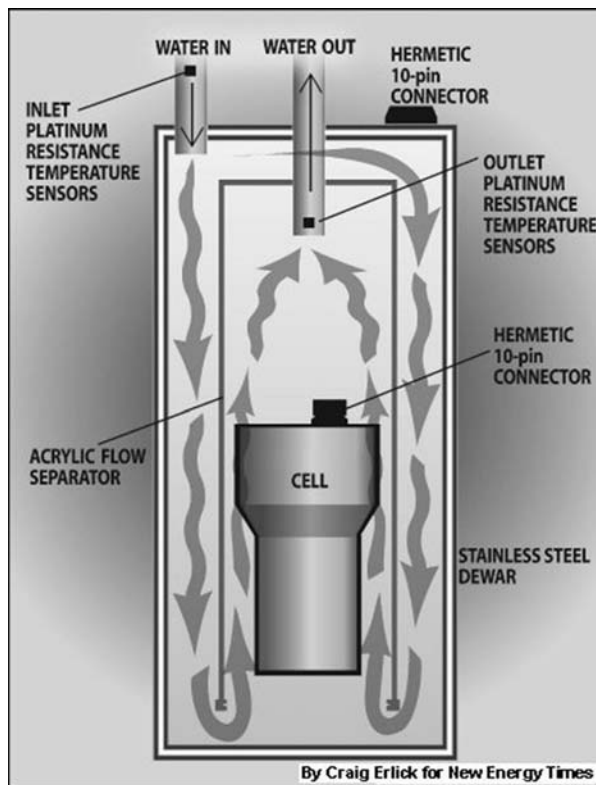


**Figure 89** Schematic of SRI International type mass-flow calorimeter. Drawing by Craig Erlick for *New Energy Times*.

experiment, which replicated the work of, among others, Debra R. Rolison and William E. O'Grady at the Naval Research Laboratory in Washington, D.C., in 1989.<sup>78,83</sup>

### **Mass-flow calorimetry**

Mass-flow calorimeters enclose the experiment in a chamber filled with a recirculating fluid or use a closely contacting heat exchanger to extract heat. The temperature of the fluid is measured when it enters the chamber and when it exits the chamber. The difference in the temperatures along with the flow rate can be used to calculate accurately the heat coming from the reaction.

Mass-flow calorimeters are practically more difficult to operate, but they have the advantage of being much easier to calibrate, and errors are easier to recognize.

However, this method constantly circulates a fluid around the cell, which promotes cooling and thereby prevents rise in temperature. If cell temperatures are allowed to increase, positive feedback occurs in LENR experiments, leading to even higher cell temperatures ([Figures 89–91](#)).



**Figure 90** ENEA glow discharge LENR cell surrounded by flow calorimetry coil.

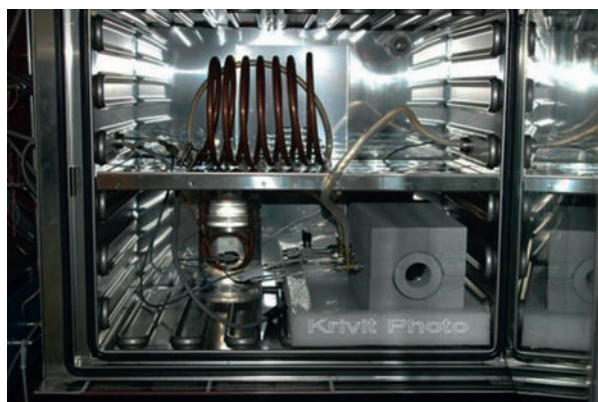


**Figure 91** Cell on bottom right, surrounded by insulation, coil and bath on top and bottom left for temperature-stabilization of calorimetry fluid.

### ***Enclosure calorimetry (Seebeck-type)***

The enclosure type of calorimeter is a thermally insulated container in which an experiment is placed. Many thermocouples are embedded within the walls of the enclosure, and they measure temperature within the container and outside the container. These data are collected and used to determine the heat generated within the container.

An advantage of the enclosure calorimeter is that it is relatively simple to use and can thereby provide more error-free and reliable results. It can also be used in parallel with a mass-flow calorimeter, fully enclosed within it, for redundant calorimetry.

### ***Isoperibolic-enclosure hybrid calorimetry***

The optimal experimental configuration to obtain high heat results uses isoperibolic calorimetry, which does not cool the cell, and takes advantage of the positive feedback effect (see below). Dash (Portland State University) and Wu-Shou Zhang (Institute of Chemistry, Chinese Academy of Sciences) explained in a 2007 paper that electrolyte temperature is a key factor in excess-heat production. They reported that they obtained their best results when the electrolyte temperature was close to the boiling point. Knowing this, they placed their entire experiment, including the isoperibolic measurement system, within a Seebeck-type enclosure calorimeter.<sup>21</sup>

## **Calorimetry Critique**

### ***Improper stirring critique***

The first critique of Fleischmann and Pons' excess-heat claims came from Nathan Lewis (Caltech) and Walter E. Meyerhof (Stanford) at the May 1989 American Physical Society meeting. Both scientists publicly stated with conviction that Fleischmann and Pons had made a sophomoric error in measuring heat in their electrochemical cells.

Specifically, both critics said that the claimed temperature gradient reported by Fleischmann and Pons in their electrochemical cell was invalid because they had neglected to use a mechanical stirrer.

Fleischmann and Pons put Lewis and Meyerhof's speculations to rest a week later in Los Angeles at the Electrochemical Society meeting with a videotaped demonstration.

The videotape showed that the natural geometry of the cell they designed, in conjunction with the bubbling action of the electrolyte, accomplished the task of stirring in seconds, without the need for a mechanical stirring device.

### ***Recombination error critique***

Another speculation that critics offered as a possible explanation for the excess-heat claim concerned the issue of recombination. As heavy water ( $D_2O$ ) dissociates within the electrolytic cell, deuterium and oxygen gases leave the cell, taking with them some chemical energy.

In order to perform a full accounting of potential excess heat, researchers must account for this energy loss. Some critics speculated that errors in such a recalculation could lead to an overcorrection and could be responsible for the claims of apparent excess heat.

The criticism became moot when most researchers switched to thermodynamically closed cells, wherein the devolving deuterium and oxygen gases were recombined, thus keeping the chemical energy fully within the cell and eliminating the need for corrective calculations.

### ***Low magnitude of heat effect critique***

Numerous examples of large effects, relative to the calorimetric uncertainty, have been reported in the literature. Calorimeters must be able to measure temperature changes precisely and maintain such precision over long periods.

The early criticisms against Fleischmann and Pons were simply uninformed. The pair had designed a calorimeter that was accurate to  $\pm 0.1$  mW for an 800 mW input. Many of their experimental runs showed excess heat in the hundreds of milliwatts.

## **General Characteristics of Low-Energy Nuclear Reactions**

### **Runaway Experiments and Self-Heating**

Several rare experimental incidents have been reported, many of them anecdotal and none of them repeatable at will. Nevertheless, some reports have been documented, and all have been of sufficient magnitude to warrant notice.

Around September 1993, before the Piantelli group published its first paper, Piantelli was running a Ni-H gas experiment. Around 7 in the evening, he looked at the monitor. Something didn't look normal; he didn't see the typical modest temperature gain and plateau. Instead, the temperature was increasing rapidly. He had already turned off heater input power.

A rapidly increasing temperature in an enclosed steel container could be a deadly problem. He wasn't sure what to do. Should he terminate the experiment, and if so, how would he stop it? He wondered whether he should leave the building. Instead, he called Focardi in Milan—at 2 in the morning—and asked, "What should I do?"

This was before Piantelli knew about the poisoning effect of deuterium. Admixtures of deuterium and hydrogen in LENR experiments don't work because each isotope oscillates at different frequencies on the surfaces of metal hydrides, and the different frequency oscillations inhibit the coherent collective effects that are required to create the heavy-mass surface plasmon electrons.

But Focardi came up with a solution: Introduce nitrogen into the cell. And it worked. It stopped the uncontrolled temperature rise and terminated the experiment (before it killed Piantelli).

Piantelli didn't know how hot the experiment had gotten before he stopped it because the monitor eventually blacked out. However, the metal thermocouples inside the cell melted. This told him that the temperature exceeded  $1450^\circ\text{C}$ . Even though he witnessed an exciting moment in science, he was understandably angry because these experiments take a long time to run and he had to abandon this one prematurely.

In the early 1990s, Mizuno reported the uncontrolled boil-off of a cell initially running 24 W of input power. After Mizuno disconnected the cell from the input power, it remained hot, and he placed it in a bucket of water. It boiled the water; he added more. This went on for 8 days. During this time, while the current was turned off, it boiled a total of 17.5 liters of water. According to his calculations of the replenished water, during the time the cell was turned off, it evaporated enough water to account for  $8.2 \times 10^7$  J of energy.

On April 11, 1992, Fleischmann and Pons did not replenish the electrolyte in a set of four cells and allowed them to run dry. They displayed a videotape of this event at a conference in Nagoya, Japan. The video displays four cells, each of them initially producing small, fine bubbles from the hydrogen evolution during the loading process. The current in the first cell was 0.500 A. The initial current in each of the other three cells was 0.200 A, which was increased to 0.500 A at the beginning of days 3, 6, and 9 of the experiment, respectively. In the course of the experiment, each cell, one by one, reaches the boiling point. The contents begin to bubble vigorously, then vaporize within minutes.

Time-lapse video of April 11, 1992, Fleischmann and Pons four-cell boil-off: <http://www.youtube.com/watch?v=mBAIIZU6Oj8>

Fleischmann and Pons were able to make power and energy calculations based on the volume of vaporized heavy water: 144 W of excess power, 86.7 MJ of excess energy for a 10-minute period and an energy density (based on the volume of the palladium cathode) of  $3.7 \text{ kW cm}^{-3}$ .

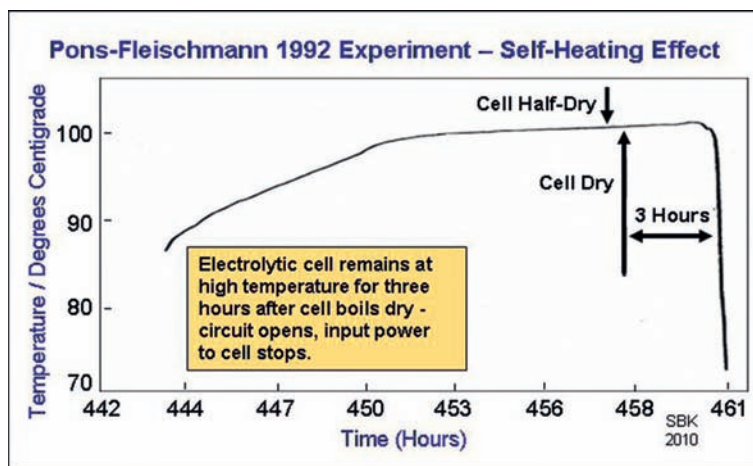


**Figure 92** Pons-Fleischmann's 1992 self-heating effect.

When the electrolytic circuit was broken as a result of the absence of the electrolyte, the cell continued to give off excess heat for 3 h. A Kel-F plastic support melted, indicating temperatures above 300 °C (Figure 92).

In the early 1990s, Mosier-Boss observed a boil-off. She said the cathode also partially vaporized. A metallurgist at her laboratory inspected the cell from that experiment using a SEM. He noted that the silver streaks seen on the sides and top of the cell appeared similar to formations he had seen only when the metal had melted under water.

### Positive Feedback

In 1993, Pons and Fleischmann reported a phenomenon in their experiments that they called a positive-feedback effect.<sup>84</sup>

"There is an element of 'positive feedback' between the increase of temperature and the rate of generation of excess enthalpy. The existence of this feedback has been a major factor in the choice of our calorimetric method and especially in the choice of our experimental protocols," the authors wrote.

In other words, as the experiments get hotter, the rate of temperature increase accelerates. This may lead to important information about the experimental parameters necessary to generate excess heat more reliably. Most experiments using the electrochemical method run at temperatures too low to take advantage of this positive feedback. One reason is that it is generally easier for experimenters to build a more precise calorimetry system that operates in the lower temperature range. A second reason, for experimenters using costly deuterium, was the financial incentive to prevent the D<sub>2</sub>O from vaporizing. However, this factor became less important after researchers widely adopted the use of recombiners, and it is not a factor for researchers using the H<sub>2</sub>O system.

Fleischmann told Miles, one of his collaborators and close colleagues, that the cell temperature needs to be above 60 °C in order to get positive feedback to produce the large excess-heat effects. According to Miles, few researchers in the field seemed to be aware of the importance of cell temperatures above 60 °C, and they used mass-flow calorimetry systems. However, these systems typically maintain cell temperatures near room temperature. For this reason, Fleischmann and Pons avoided mass-flow calorimetry.

In 1998, Mengoli also reported running experiments at 95 °C with great success.

"The major achievement of this work is to have devised the temperature range in which the generation of excess power is a totally reproducible phenomenon," Mengoli wrote.<sup>85</sup>

Mengoli also reported a period in which an experiment produced power in the absence of any power input, after the electrolytic circuit had been opened.

The gamma conversion to infrared, according to the Widom-Larsen theory, helps explain the positive-feedback phenomenon and the potential of experiments to be self-sustaining. Larsen explained that the Piantelli experiment — the hydrogen gas experiment housed in a stainless steel chamber — is an example of a resonant electromagnetic cavity in which the infrared radiation is strongly reflected from the walls of the cell and causes positive thermal feedback.

"The gammas are converted into infrared, and the walls re-radiate the infrared back into the active area of the experiment," Larsen said. "If they didn't convert, the gammas would go right through the stainless steel walls and escape, and they would cool the system."

According to Larsen, the Piantelli experiment provides an easy way to understand the natural ability of LENRs to self-sustain. Getting the system to start requires the addition of enough energy to create the first neutrons. The Piantelli design does this with an electric heater. Once the system gets going, it starts emitting electromagnetic radiation in the form of infrared heat. It reflects back from the stainless steel walls and feeds the production of the neutrons. Once the cycle starts, because the net energy gain is positive, the system doesn't need the electric heater, and it runs until the fuel is consumed.

Larsen performed a simple calculation based on one proposed nucleosynthetic pathway, predicting that this type of experiment should produce an eightfold gain of energy.

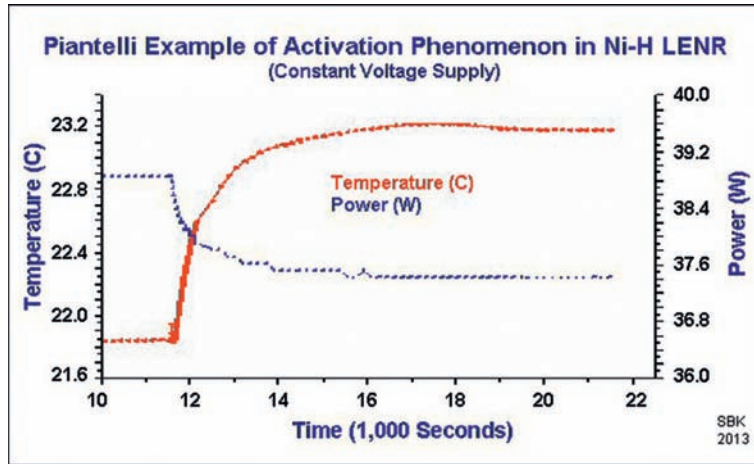


Figure 93 Piantelli example of activation phenomenon in Ni-H LENR.

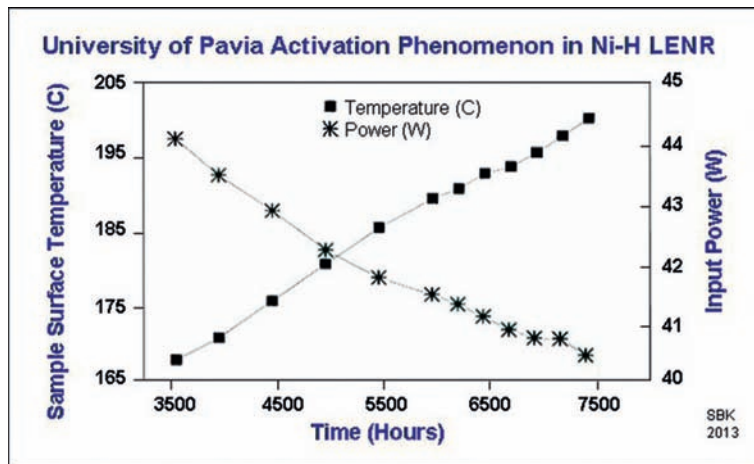


Figure 94 University of Pavia replication of Piantelli activation phenomenon in Ni-H LENR.

In September 2010, at the 9th International Workshop on Anomalies in Hydrogen/Deuterium Loaded Metals in Pontignano, Siena, Piantelli displayed the typical inverse relationship between input power and cell temperature in his Ni-H LENR cells. He said pressure and voltage remain constant. After a period during which the hydrogen is loaded into the nickel, and power and temperature remain constant, an activation occurs. Temperature begins to rise sharply even though power is reduced (Figure 93).<sup>86</sup>

Piantelli displayed a similar activation phenomenon in a replication that was performed by Luigi Nosenzo (University of Pavia) and Luigi Cattaneo, of Consiglio Nazionale Ricerche (National Research Council), at the University of Pavia (Figure 94).

### Materials Science Challenges

The greatest experimental challenge facing researchers in the field today is creating the materials, conditions and stimuli that consistently produce excess heat reactions. With rare exceptions, the ability to create heat reactions on demand has been elusive. The Widom-Larsen theory, however promising in explaining the anomalies, does not provide instructions on how to create the required conditions for successful experiments.

Widom and Larsen's paper "Theoretical Standard Model Rates of Proton to Neutron Conversions Near Metallic Hydride Surfaces" does offer researchers a suggestion.

"Successful fabrication and operation of long-lasting energy-producing devices with high percentages of nuclear active surface areas will require nanoscale control over surface composition, geometry and local field strengths," the authors wrote.

The loading ratio of deuterium or hydrogen into the metal of at least 0.90 is known to be crucial, and some researchers, particularly those using co-deposition, have made progress in loading. But there is still a long way to go to obtain fully repeatable,

reproducible, practical levels and sustained heat. The involvement of metallurgists, materials scientists and nanotechnology experts is essential to the developing field.

In the recorded experiments, the reaction sites do not appear to be uniformly distributed across the test samples. Instead, the sites appear to be scattered among multiple, randomly distributed spots that are significantly smaller than the overall sample.

### Technology Readiness of LENR

A variety of organizations throughout the world uses the term Technology Readiness Level (TRL) to help identify the progress of newly introduced ideas and science as they become ready for practical applications. Like many new ideas, LENR could lead to world-changing energy technologies. But LENR has a long way to go before it is a practical technology. The science must be understood first, and, in general, it is not. This places LENR at the very bottom of all TRL scales. Mizuno spoke about the potential of LENRs at the American Chemical Society meeting in Salt Lake City on March 22, 2009.

"If the LENR transmutation mechanism can be understood," Mizuno said, "it may then be possible to control the reaction and perhaps produce macroscopic quantities of rare elements by this method. In the distant future, industrial-scale production of rare elements might become possible, and this would help alleviate material shortages worldwide."

Since 1989, a variety of companies, most of them no longer in existence, have claimed to be very close to a practical LENR technology. In every case, all were still at the bottom of any TRL scale. Nevertheless, the prospects of LENR technologies have attracted a fair number of people, both researchers and investors, many of whom have made premature claims of possessing LENR reactor technology. It is certainly extraordinary that chemistry and other low-energy experiments can lead to nuclear reactions. Nevertheless, an expansive database exists to support the validity of the field. Despite that scientific validity, new participants should use great caution when considering claims that are far beyond the current state of the art in LENRs.<sup>87</sup>

LENRs may lead to a new gold rush, and people who are prepared and skilled will have the greatest advantages. People who rush into the field as speculators, without clearly understanding the existing science and challenges, will almost certainly find nothing. In the last few years, events have shown that even a few scientists with respectable credentials have lost their objectivity. Until LENR products can be purchased in the open marketplace, the only reliable method to differentiate valid from invalid claims is science, performed carefully, reported in detail, and published openly.

### Conclusion

All of the observed reactions appear to lack significant high-flux neutron and gamma ray emissions. Therefore, they show promise as the basis of a new science that would enable new types of nuclear power systems that would not need complex containment or disposal systems. Low levels of radiation are found in at least some of these reactions, but this radiation is usually absorbed directly and promptly within the experiments. Consequently, they offer hope of practical applications, such as heating and electrical generation, that do not pose major health hazards or compromise the environment.

In addition to their lack of high-flux radiation, the experiments do not appear to produce any greenhouse gases or long-lived radioactive decay emissions.

Moreover, recent experiments suggest the possibility of using the transmutation reactions to clean up the radioactive material that results from nuclear fission reactions.

### References

1. Fleischmann, M.; Pons, S. J. *Electroanal. Chem.* **1989**, *261*, 301–308, Errata M. Fleischmann; Pons, S.; Hawkins, M. **1989**, *263*, 187–188.
2. *New Energy Times*, 'University of Utah Fusion Press Conference' <http://newenergytimes.com>.
3. Wendt, G. L.; Irion, C. E. *J. Am. Chem. Soc.* **1922**, *44*, 1887–1894.
4. Coehn-Göttingen, A. *Zeitschrift für Elektrochemie* **1929**, *35*, 676.
5. Bridgman, P. W. *The Physics of High Pressure*; International Textbooks of Exact Science: London, 1947.
6. Widom, A.; Larsen, L. *Eur. Phys. J. C* **2006**, *46*, 107–110.
7. Hull, L. Letter. *Chemical and Engineering News*, May 15, 1989.
8. Widom, A.; Larsen, L. Apparatus and Method for Absorption of Incident Gamma Radiation and its Conversion to Outgoing Radiation at Less Penetrating, Lower Energies and Frequencies. U.S. Patent Appl. 7,893,414, 2011.
9. Larsen, L. Slide Presentation, February 7, 2009, [www.slideshare.com](http://www.slideshare.com).
10. Nuclides 2000 Program. Lide, D. R., Ed.; *Handbook of Chemistry and Physics*, 81st ed.; CRC Press: Boca Raton, FL, 2000–2001.
11. Larsen, L. Slide Presentation, March 22, 2013, [www.slideshare.com](http://www.slideshare.com).
12. Focardi, S.; Gabbani, V.; Montalbano, V.; Piantelli, F.; Veronesi, S. *Il Nuovo Cimento* **1998**, *111A*, 1233–1242.
13. *New Energy Times*, Piantelli Group LENR News and Research Papers. <http://newenergytimes.com>.
14. Campari, E.; Focardi, S.; Gabbani, V.; Montalbano, V.; Piantelli, F.; Veronesi, S. Overview of H-Ni Systems: Old Experiments and New Setup. In *5th Asti Workshop on Anomalies in Hydrogen-Deuterium-Loaded Metals, Asti, Italy*, 2004.
15. Widom, A.; Larsen, L. 'Theoretical Standard Model Rates of Proton to Neutron Conversions Near Metallic Hydride Surfaces', <http://arxiv.org/abs/nucl-th/0608059v2> September 25, 2007.
16. Larsen, L. Slide Presentation, June 25, 2009, [www.slideshare.com](http://www.slideshare.com).

17. Larsen, L. *Portable and Distributed Power Generation from LENRs*; Institute of Science in Society: London, 2008.
18. Larsen, L. Slide Presentation, September 27, 2011, [www.slideshare.com](http://www.slideshare.com).
19. Roulette, T.; Roulette, J.; Pons, S. In Proceedings of the Sixth International Conference on Cold Fusion: Progress in New Hydrogen Energy, Hokkaido, Japan, October 13–18, 1996; Okamoto, M., Ed.; New Energy and Industrial Technology Development Organization, Tokyo, 1996.
20. Miley, G. In ICCF8: Proceedings of the Eighth International Conference on Cold Fusion, Lerici (La Spezia), Italy, May 21–26, 2000; Scaramuzzi, F., Ed.; Italian Physical Society, Bologna, 2001.
21. Zhang, W.-S.; Dash, J. In Condensed Matter Nuclear Science: Proceedings of the 13th International Conference on Condensed Matter Nuclear Science, Sochi, Russia, June 25–July 1, 2007; Bazhutov, Y., Ed.; Publisher Center MATI, Tsiolkovsky Moscow Technical University, Moscow, 2008.
22. Letts, D.; Cravens, D. In Condensed Matter Nuclear Science: Proceedings of the 10th International Conference on Cold Fusion, Cambridge, MA, August 24–29, 2003; Hagelstein, P. L.; Chubb, S. R., Eds.; World Scientific, Singapore, 2006.
23. Violante, V.; Castagna, E.; Sibilia, C.; Paoloni, S. In Condensed Matter Nuclear Science: Proceedings of the 10th International Conference on Cold Fusion, Cambridge, MA, August 24–29, 2003; Hagelstein, P. L.; Chubb, S. R., Eds.; World Scientific, Singapore, 2006.
24. Arata, Y.; Chang, Z.-Y. *Koon Gakkai Shi (J. High Temp. Soc.)* **1994**, *20*, 148–155.
25. Mizuno, T.; Ohmori, T.; Akimoto, T.; Takahashi, A. *Jpn. J. Appl. Phys.* **2000**, *39*, 6055.
26. Cirillo, D.; Iorio, V. In Condensed Matter Nuclear Science: Proceedings of the 11th International Conference on Cold Fusion, Marseilles, France, October 31–November 5, 2004; Biberian, J.-P., Ed.; World Scientific, Singapore, 2006.
27. Mosier-Boss, P. A.; Szpak, S.; Gordon, F. E.; Forsley, L. P. G. Detection of Energetic Particles and Neutrons Emitted during Pd:D Co-deposition. In *Low Energy Nuclear Reactions Sourcebook*; Marwan, J.; Krivit, S. B., Eds.; American Chemical Society: Washington, DC, 2008; pp 311–334.
28. Miles, M. In Proceedings of the Seventeenth International Conference on Cold Fusion, Daejeon, Korea, 2012.
29. Miley, G. H.; Patterson, J. *J. New Energ.* **1996**, *1*, 5.
30. Miley, G. H.; Hora, H.; Lipson, A.; Kim, S.-O.; Luo, N.; Castano, C. H.; Woo, T. In Condensed Matter Nuclear Science: Proceedings of the 9th International Conference on Cold Fusion, Beijing, China, May 19–24, 2002; Li, X. Z., Ed.; Tsinghua University Press, Beijing, 2002.
31. Paneth, F.; Peters, K. *Naturwissenschaften* **1926**, *14*, 956–962.
32. Arata, Y.; Chang, Z.-Y. *J. High Temp. Soc.* **2008**, *34*.
33. Savvatimova, I. B.; Kucherov, Y.; Karabut, A. B. Cathode Material Change after Deuterium Glow Discharge Experiments. *T. Fusion Technol.* **1994**, vol. 20, (Chapter 4T), 389–394.
34. Savvatimova, I. B.; Gavritenkov, D. In Condensed Matter Nuclear Science: Proceedings of the 11th International Conference on Cold Fusion, Marseilles, France, October 31–November 5, 2004; Biberian, J.-P., Ed.; World Scientific, Singapore, 2006.
35. Iwamura, Y.; Sakano, M.; Itoh, T. *Jpn. J. Appl. Phys.* **2002**, *41*, 4642–4650.
36. Higashiyama, T.; Sakano, M.; Miyamaru, H.; Takahashi, A. In Condensed Matter Nuclear Science: Proceedings of the 10th International Conference on Cold Fusion, Cambridge, MA, August 24–29, 2003; Hagelstein, P. L.; Chubb, S. R., Eds.; World Scientific, Singapore, 2006.
37. Biberian, J.-P.; Armanet, N. In Condensed Matter Nuclear Science: Proceedings of the 13th International Conference on Condensed Matter Nuclear Science, Sochi, Russia, June 25–July 1, 2007; Bazhutov, Y., Ed.; Publisher Center MATI, Tsiolkovsky Moscow Technical University, Moscow, 2008.
38. Fralick, G. C.; Decker, A. J.; Blue, J. W. In NASA Technical Memorandum 102430, Cleveland, OH, December, 1989.
39. Kortkhonjia, V. P. *Tech. Phys. Lett.* **2003**, *29*, 797–800.
40. Adamenko, S.V. In Proton-21 corporate document, 2004. <http://www.proton21.com.ua>
41. Adamenko, S. V.; Selli, F.; Van Der Merwe, A. *Controlled Nucleosynthesis: Breakthroughs in Experiment and Theory. Fundamental Theories of Physics*; Springer: Berlin, 2007; Vol. 156, p 780.
42. Stringham, R. S. Sonofusion, Deuterons to Helium Experiments. In *American Chemical Society Symposium Series: Low-Energy Nuclear Reactions and New Energy Technologies Sourcebook*; Marwan, J.; Krivit, S. B., Eds.; American Chemical Society/Oxford University Press: Washington, DC, 2009; Vol. 11, pp 159–173.
43. Vysotskii, V. I.; Kornilova, A. A. *Nuclear Transmutation of Stable and Radioactive Isotopes in Biological Systems*; Pentagon Press: New Delhi, 2009.
44. Mizuno, T.; Akimoto, T.; Azumi, K.; Kazuya, K.; Kurokawa, M.; Enyo, M. *Fusion Technol.* **1996**, *29*, 385–389.
45. Biberian, J.-P. In Proceedings of the 5th International Conference on Cold Fusion, Monte Carlo, Monaco, April 9–13, 1995; Pons, S., Ed.; IMRA Europe, Sophia Antipolis Cedex, France, Monte Carlo, 1995.
46. Singh, M.; Saksena, M.; Dixit, V.; Kartha, V. *Fusion Technol.* **1994**, *26*, 266–270.
47. Mizuno, T. *J. Environ. Sci. Eng.* **2011**, *5*, 453–459.
48. Mizuno, T. *Isotopic Changes of Elements Caused by Various Conditions of Electrolysis*; American Chemical Society: Salt Lake City, UT, 2009.
49. Bush, B.F.; Lagowski, J.J. Trace Elements Added to Palladium by Electrolysis in Heavy Water; Machiels, A. and Passell, T. Project Managers; EPRI TP-108743, November 1999.
50. Passell, T. O. In Condensed Matter Nuclear Science: Proceedings of the 10th International Conference on Cold Fusion, Cambridge, MA, August 24–29, 2003; Hagelstein, P. L.; Chubb, S. R., Eds.; World Scientific, Singapore, 2006.
51. Passell, T. O. In Proceedings of the Sixth International Conference on Cold Fusion: Progress in New Hydrogen Energy, Hokkaido, Japan, October 13–18, 1996; Okamoto, M., Ed.; New Energy and Industrial Technology Development Organization, Tokyo, 1996.
52. Qiao, G. S.; Han, X. L.; Kong, L. C.; Zheng, S. X.; Huang, H. F.; Yan, Y. J.; Wu, Q. L.; Deng, Y.; Lei, S. L.; Li, X. Z. In Proceedings of the Seventh International Conference on Cold Fusion, Vancouver, BC, Canada, April 19–24, 1998, ENCO: University of Utah Research Park, 1998.
53. Miley, G.; Narne, G.; Woo, T. *J. Radiolog. Nucl. Chem.* **2005**, *263*, 691.
54. Lipson, A. G.; Roussetski, A. S.; Miley, G. H.; Castano, C. H. In Condensed Matter Nuclear Science: Proceedings of the 9th International Conference on Cold Fusion, Beijing, China, May 19–24, 2002; Li, X. Z., Ed.; Tsinghua University Press, Beijing, 2002.
55. Srinivasan, M. Observation of Neutrons and Tritium in a Wide Variety of LENR Configurations: BARC Results Revisited. In 237th American Chemical Society National Meeting, Salt Lake City, UT, March, 2009.
56. Forsley, L.P.G.; Mosier-Boss, P.; Phillips, G.W.; Szpak, S.; Khim, J.W.; Gordon, F.E., Presented at American Physical Society, Denver, CO, March 5, 2007. <http://newenergytimes.com/v2/library/2007/2007ForsleyL-APS.pdf>
57. Szpak, S.; Mosier-Boss, P. A.; Miles, M. H.; Fleischmann, M. *Thermochem. Acta* **2004**, *410*, 101–107.
58. Tanzella, F.; Earle, B. P.; McKubre, M. C. H. In Eighth International Workshop on Anomalies in Hydrogen/Deuterium Loaded Metals, Catania, Italy, October 13–18, 2007.
59. Cirillo, D. *T. Am. Nucl. Soc.* **2012**, *107*, 418–421.
60. Iyengar, P. K. In Proceedings of the Fifth International Conference on Emerging Nuclear Energy Systems, Karlsruhe, Germany, July 3–6, World Scientific Publishing Co. Pte. Ltd., 5 Toh Tuck Link, Singapore 596224, 1989.
61. Packham, N. J. C.; Wolf, K. L.; Wass, J. C.; Kainthla, R. C.; Bockris, J. O' M. J. *Electroanal. Chem.* **1989**, *289*, 451.
62. Clarke, B. W.; Oliver, B. M.; McKubre, M. C. H.; Tanzella, F.; Tripodi, P. *Fusion Sci. Technol.* **2001**, *40*, 152.
63. McKubre, M. C. H. Condensed Matter Nuclear Science: Proceedings of the 10th International Conference on Cold Fusion, Cambridge, MA, August 24–29, 2003; Hagelstein, P. L.; Chubb, S. R., Eds.; World Scientific, Singapore, 2006.
64. Claytor, T. N.; Jackson, D. D.; Tuggle, D. G. *Tritium Production From a Low Voltage Deuterium Discharge on Palladium and Other Metals*. Los Alamos National Laboratory: Los Alamos, NM, 2002.
65. Claytor, T. N.; Schwab, M. J.; Thoma, D. J.; Teter, D. F.; Tuggle, D. G. In Proceedings of the Seventh International Conference on Cold Fusion, Vancouver, BC, Canada, April 19–24, 1998, ENCO: University of Utah Research Park, 1998.

66. Bush, B. F.; Lagowski, J. J.; Miles, M. M.; Ostrom, G. S. *J. Electroanal. Chem.* **1991**, *304*, 271–278.
67. Miles, M. M.; Bush, B. F.; Lagowski, J. J. *Fusion Technol.* **1994**, *25*, 478.
68. McKubre, M.; Tanzella, F.; Tripodi, P.; Hagelstein, P. In: Proceedings of the Eighth International Conference on Cold Fusion, Lerici (La Spezia), Italy, May 21–26, 2000; Scaramuzzi, F., Ed.; Italian Physical Society: Bologna, 2001.
69. Larsen, L. Slide Presentation, slide #37, September 3, 2009, [www.slideshare.com](http://www.slideshare.com).
70. Miley, G. H.; Shrestha, P. J. In Condensed Matter Nuclear Science: Proceedings of the 10th International Conference on Cold Fusion, Cambridge, MA, August 24–29, 2003; Hagelstein, P. L.; Chubb, S. R., Eds.; World Scientific, Singapore, 2006.
71. Mizuno, T.; Ohmori, T.; Akimoto, T.; Kurokawa, K.; Kitaichi, M.; Inoda, K.; Azumi, K.; Simokawa, S.; Enyo, M. In Proceedings of the Sixth International Conference on Cold Fusion: Progress in New Hydrogen Energy, Hokkaido, Japan, October 13–18, 1996; Okamoto, M., Ed.; New Energy and Industrial Technology Development Organization, Tokyo, 1996.
72. Widom, A.; Larsen, L. 'Nuclear Abundances in Metallic Hydride Electrodes of Electrolytic Chemical Cells', February 20, 2006, <http://arxiv.org/abs/cond-mat/0602472>.
73. Iwamura, Y. *T. Am. Nucl. Soc.* **2012**, *107*, 422–425.
74. Larsen, L. Slide Presentation, February 12, 2012, [www.slideshare.com](http://www.slideshare.com).
75. Szpak, S.; Mosier-Boss, P. A.; Dea, J.; Gordon, F. E. In Condensed Matter Nuclear Science: Proceedings of the 10th International Conference on Cold Fusion, Cambridge, MA, August 24–29, 2003; Hagelstein, P. L.; Chubb, S. R., Eds.; World Scientific, Singapore, 2006.
76. Szpak, S.; Mosier-Boss, P. A.; Young, C.; Gordon, F. E. *Naturwissenschaften* **2005**, *92*, 394–397.
77. Ohmori, T.; Mizuno, T.; Enyo, M. In Proceedings of the Sixth International Conference on Cold Fusion: Progress in New Hydrogen Energy, Hokkaido, Japan, October 13–18, 1996; Okamoto, M., Ed.; New Energy and Industrial Technology Development Organization, Tokyo, 1996.
78. Valat, M. M.S. Thesis, Portland State University, Portland, OR, 2011.
79. Mengoli, G.; Bernardini, M.; Manducchi, C.; Zannoni, G. *Il Nuovo Cimento* **1998**, *20D*, 331–352.
80. Krivit, S.B. Deuterium and Palladium Not Required. *New Energy Times*, July 10, 2008.
81. Krivit, S.B. Piantelli-Focardi Publication and Replication Path. *New Energy Times*, July 10, 2008.
82. McKubre, M. Private Communications, January 20, 2009.
83. Rolison, D. R.; O'Grady, W. E. In Proceedings: EPRI-NSF Workshop on Anomalous Effects in Deuterided Metals, Washington, D.C., October 16–18, 1989, Published by Electric Power Research Institute EPRI, 1993.
84. Fleischmann, M.; Pons, S. *Phys. Lett. A* **1993**, *176*, 118.
85. Mengoli, G.; Bernardini, M.; Manducchi, C.; Zannoni, G. *J. Electroanal. Chem.* **1998**, *444*, 155.
86. Piantelli, F. Proton Reactor. In 9th International Workshop on Anomalies in Hydrogen/Deuterium Loaded Metals, Pontignano, Siena, Italy, 2010.
87. *New Energy Times*, LENR Companies and Commercial New Energy Research, <http://newenergytimes.com>.